Materials Advances

ROYAL SOCIETY OF CHEMISTRY

REVIEW

View Article Online
View Journal | View Issue

Cite this: *Mater. Adv.*, 2022, 3, 2670

A journey of thermoplastic elastomer nanocomposites for electromagnetic shielding applications: from bench to transitional research

Ankur Katheria, Jasomati Nayak and Narayan Ch. Das *

Received 23rd October 2021,
Accepted 2nd February 2022

DOI: 10.1039/d1ma00989c

rsc.li/materials-advances

The rapid growth and day to day skyrocketing use of electronic equipment and gadgets used across a vast spectrum of industrial, military, consumer, and commercial sectors have led to a meteoritic rise in a new type of electronic pollution such as electronic noise, radiofrequency interference (RFI), and electromagnetic interference (EMI) which leads to the interference or malfunctioning of the electronic equipment. Studies in the past revealed that metals and their alloys, dielectric ceramics, and semiconductors are promising candidates for EMI shielding materials but their high cost, heavy weight, and low corrosion resistance have narrowed their application. On the other hand, polymer composites are easy to fabricate, more economical, and corrosion-resistant. Although inherently being insulators, these polymer composites can be made conductive by adding conductive fillers to the polymer matrix to increase their electrical conductivity. This review paper reports the application of conductive thermoplastic elastomer (TPE) nanocomposites in the shielding of electromagnetic interference.

1 Introduction

In the past few decades electromagnetic interference has become a matter of great concern affecting our day-to-day life terribly owing to the rapid evolution of technology and global usage of electronic gadgets.[1–5] Electromagnetic interference is the electromagnetic pollution or signal that can result from any man-made device (computer circuits, arc welders, brush motors, *etc.*) or natural source (lightning, solar magnetic storms, earth's magnetic field flux, *etc.*). A higher electronic wave frequency potentially disrupts the performance of sensitive electronic equipment and devices with effects ranging from short-term disturbances to permanent system failures.[6,57]

Rubber Technology Centre, Indian Institute of Technology, Kharagpur 721302, India. E-mail: ncdas@rtc.iitkgp.ac.in

Ankur Katheria

Mr Ankur Katheria completed his Bachelor of Technology in Plastic Technology at CIPET (Lucknow), Uttar Pradesh, India, in 2015, and Master of Technology in Materials Science at IIT Kharagpur, West Bengal, India, in 2019. He is currently a doctoral candidate in the Rubber Technology Center at IIT Kharagpur, West Bengal, India, under the supervision of Dr Narayan Chandra Das. His research focus includes polymer nanocomposites for the application of EMI shielding.

Jasomati Nayak

Mrs Jasomati Nayak is a PhD scholar in the Rubber Technology Centre, Indian Institute of Technology Kharagpur, West Bengal, India, under the supervision of Dr Narayan Chandra Das. She received her Master of Technology degree in Material Science and Chemical Technology from the Department of Applied Chemistry at the Defence Institute of Advanced Technology, Pune, Maharashtra, India, in 2019 and Bachelor of Technology degree in Plastic Engineering from the Central Institute of Plastic Engineering and Technology, Bhubaneswar, Odisha, in 2014. Her current research focus includes thermoplastic elastomer materials and polymer nanocomposites towards EMI shielding application.

The adverse effects of EMI are not only limited to the malfunctioning of electronic appliances; they also pose a significant threat to biological lifeforms. Constant exposure to electromagnetic radiation increases the chances of life-threatening conditions such as heart problems, asthma, cancer, and even miscarriages.[7–11]

Previous research studies have proved that conducting or magnetic materials such as metals, conducting polymers, carbon-based materials, dielectric, and magnetic materials can be effectively used to block the penetration of EM radiation.[12–17,58] Traditionally, metals and metallic composite materials have been used for EMI shielding, but their applications are confined by their heavyweight, poor mechanical flexibility, high density, corrosiveness, and high processing costs.[18–22] Thus, active research has been ongoing towards fabricating light-weight, flexible, and corrosion-resistant materials such as polymer matrix composites, which can be effective in EMI shielding applications with low processing cost.[23–32] Although some polymers are conductive, most of them are insulating by nature, and thus additives are needed in the polymer matrix to generate conductivity of the polymer composites. Carbon nanofibers,[33–35] single-walled carbon nanotubes (SWCNTs),[36–39] multi-walled carbon nanotubes (MWCNTs),[40–44] graphene,[45–48,54] *etc.* have proved to be valuable nanofillers in polymer composites. These polymer composites give designer flexibility and offer significant benefits over traditionally used metals, unfilled resins, and coatings.

From an industrial point of view, EMI is related to technical problems. Most electronic devices in operation emit electromagnetic waves, and all electronic devices are prone to EMI problems; and as a result, ensuring electromagnetic compatibility becomes necessary. In order to ensure the performance requirements, EMC regulations have been established and standards set by international organizations.[49] These standards must be satisfied for commercial electronics, and one way to achieve the EMC required level is to use shielding materials. Therefore, in a global context, the interest in investments to develop advanced materials capable of, for example, reflecting or absorbing electromagnetic radiation to overcome the crescent electromagnetic pollution is evident. Consequently, lots of research studies are being conducted with the aim of developing multifunctional shielding materials[55,56] that may present suitable mechanical properties, lower density, good processability, and, at the same time, fully satisfy aesthetics parameters.

In general, composites based on conventional thermoplastic polymers and carbon nanoparticles appear as candidates to meet most of these advanced requirements. However, EMI shielding materials must also mandatorily present flexible properties for some applications. Currently, composites based on conventional rubbers and traditional carbon particles are the most flexible EMI shielding materials. However, these composites present some significant drawbacks mainly related to the curing process and the need of a high amount of conducting fillers. Therefore, the development of materials that combine the outstanding properties of thermoplastic elastomers and carbon nanoparticles may be a promising option for developing a new generation of high-performance flexible EMI shielding materials.

Narayan Ch. Das

Dr Narayan Chandra Das is an Associate Professor in the Rubber Technology Centre at IIT Kharapgur. He received his BSc degree in Chemistry (honours) from the University of Calcutta in 1992 and BTech degree in Polymer Science and Technology from Calcutta University (1996). Subsequently, he completed his MTech degree (1998) in Rubber Technology and PhD (2002) in Polymer Science at Indian Institute of Technology Kharagpur (IIT Kharagpur), India. He carried out his post-doctoral research at Hiroshima University in Japan and Michigan Technological University in USA. He worked as a Research Associate at SUNY Binghamton in USA. He also worked as a Research Professor at Indiana University, Bloomington, USA. His interdisciplinary research areas include nanomaterials, conductive nanocomposites and EMI shielding, thermoplastics elastomers, polymer nanocomposites, rheology and processing of rubber, drug delivery, biomaterials, carbon dots, membrane for water purification, food packaging, SAXS and SANS.

2 Basic mechanism of EMI shielding

EMI shielding is the phenomenon of protecting the signals from being affected by external electromagnetic noise using manufacturing techniques or materials which can act as a barrier between the device and the surrounding component. The materials used for EMI shielding give immunity to the sensitive components in devices from incoming interference and also prevent noise from reaching other susceptible equipment.[56,59,60]

The total EMI SE_T for an EMI shielding material is contributed by three mechanisms mainly; absorption (SE_A), reflection (SE_R), and multiple internal reflections (SE_{MR}). (Fig. 1)

$$SE_T = SE_A + SE_R + SE_{MR} \quad (1)$$

The phenomenon of absorption is associated with the dissipation of the energies, whereas the surface reflection is a result of impedance mismatching of the shielding material and approaching EM wave. The multiple reflections, on the other hand, are calculated by radiation scattering inside the shielded material, which happens because of the inhomogeneity within the material.[50] However, SE_A equal to or higher than 15 dB is generally considered to be sufficiently high for the multiple reflection component not to be considered, and the shielded materials are regarded as electrically thin.[51–53]

The reflective nature of an EM wave is directly related to the surface charge in the material for which the material is required to be conducting in nature. The incident waves which

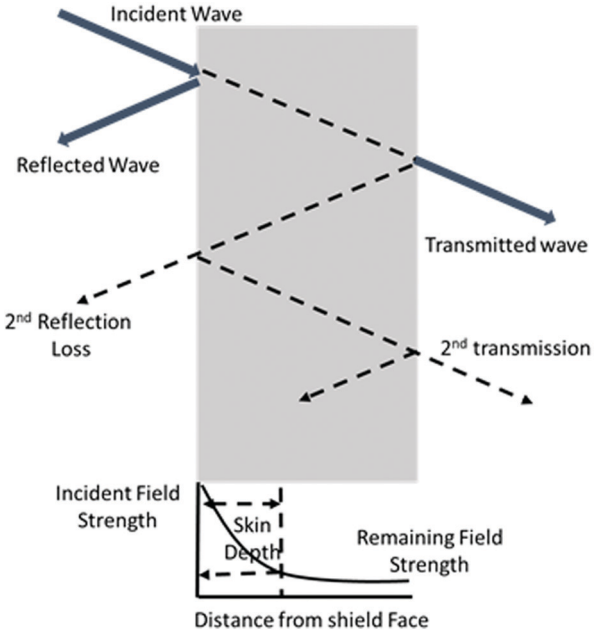

Fig. 1 Schematic representation of the EMI shielding mechanism.

are not reflected are transmitted through the medium and are dissipated as energy by absorption.[63,65] Therefore, it is important to quantify the amplitude of a transmitted EM wave. The amplitude of the wave is $e^{-z/\delta}$; where z is the distance until the EM wave penetrates into the conductive material and δ is the skin depth of the conductive material. Skin depth is defined as the distance within the conductive material where the power of the EM wave decreases by a factor $1/e$ as the EM wave transmitted goes deeper inside. Skin depth can be calculated as[67,68]

$$\delta = 1/\sqrt{\pi\omega\mu\sigma} \quad (2)$$

where ω is frequency, μ is the relative magnetic permeability of shielding materials and σ is the electrical conductivity of shielding materials. The above equation shows that skin depth has an inverse relation with electric conductivity, magnetic permeability, and frequency. Thus, an increase in the magnitude of electric conductivity, magnetic permeability and frequency will increase the reflection rather than absorption.[69]

The losses associated with reflection and multiple internal reflection are dependent on the impedance and therefore, their value varies for the electric field, magnetic field, and plane wave. Contrarily, the absorption losses will be the same for all three fields as the absorption phenomenon does not depend on the impedance.[70]

2.1 EMI shielding effectiveness (SE)

The shielding effectiveness (SE) of the material is defined as the ratio of the incidence field strength to the transmitted field strength. The shielding effectiveness in decibels (dB), is given as[71]

$$SE_P = 10\log 10(P_{in}/P_{out}) \quad (3)$$

$$SE_E = 20\log 10\,(E_{in}/E_{out}) \quad (4)$$

$$SE_H = 20\log 10\,(H_{in}/H_{out}) \quad (5)$$

where P represents the energy field, E represents the electrical field, and H represents the magnetic field. The subscripts in and out represent the magnitude of the field strength that is incident on and transmitted through the EMI shielding materials, respectively. All electromagnetic waves propagate at a right angle to the plane containing electric field and magnetic field, which are orthogonal to each other. Its characteristic depends on its frequency and associated photon energies. The ratio between the electric field strength and the magnetic field strength is called wave impedance. Based on the distance (r) of the EMI shielded material from an EM wave source, the regime of measurement is separated into the far-field and the near field. The far-field region is determined by the condition when the distance (r) is greater than $\lambda/2\pi$ between the EM wave source and shielding material. In this, for the field region, EM wave impedance is equal to the intrinsic impedance of free space [$Z_0 = [\mu_0/£_0]^{\frac{1}{2}} = 377\ \Omega$] where $\mu_0 = 4\pi \times 10^{-7}$ H m^{-1} is the permeability of free space and $£_0 = 10^7/(4\pi c^2)$ F m^{-1} is the permittivity of free space (where $c = 2.998 \times 10^8$ m/s is the velocity of light). In the near field region, the distance (r) between the EM wave source and shielding material is less than $\lambda/2\pi$.[72–75]

2.1.1 Shielding by reflection (SE_R). The primary mechanism of EMI shielding is reflection. Reflection loss (SE_R) is related to the relative impedance mismatching between the surface of the shielding material and the EM waves. The magnitude of reflection depends upon the surface conductivity and can be expressed as

$$SE_R = -10\log_{10} + 10\log\,(\sigma_T/16\omega\varepsilon_0\mu_r) \quad (6)$$

where σ_T is the total conductivity of the shielding material, and μ_r is the relative permeability. Therefore, shielding by reflection is a function of the conductivity and the permeability of the shielding materials.[76–78]

2.1.2 Shielding by absorption (SE_A). Absorption is the secondary mechanism in EMI shielding. Unlike metals, where shielding is primarily due to reflection, for polymer nanocomposites, shielding is driven by absorption,[64,66] which helps in controlling EM smog. Thus, shielding by absorption is mainly due to the current generated in the material (Ohmic losses) and magnetic hysteresis losses. For homogeneous materials, shielding by absorption can be calculated by

$$SE_A = 8.7d/\delta = 8.7d\sqrt{\pi f\mu\sigma} \quad (7)$$

where d is the thickness of the shielding material and δ is the skin depth. Hence, shielding by absorption is directly proportional to the thickness of the shielding material. Shielding by absorption increases with an increase of incident frequency, while shielding by reflection decreases with an increase of incident frequency.[79–82]

2.1.3 Shielding by multiple reflections (SE_{MR}). For thinner materials, radiation is trapped between two boundaries due to multiple reflection, *i.e.*, EM waves reflect from the second boundary, come back to the first boundary and are re-reflected from the first to second boundary, and so on. Shielding due to

multiple reflections can be estimated by the following equation if skin depth > material thickness,

$$SE_{MR} = 20 \log 10(1 - e^{-2d/\delta}) \quad (8)$$

This shielding by multiple reflections can be neglected when the thickness of the shielding material is greater than the skin depth (δ) as the amplitude of the absorbed wave becomes negligible by the time it crosses the boundary. In other words, the SE_{MR} of the shielding material is negligible if SE_A is $\geq$10 dB.[83–85]

2.2 Shielding mechanism of polymer composites

To understand the EM shielding behaviour of the composite material, it is important to study all the aspects related to it. There are many efficient media theories (EMT) providing homogenization of composite media. The Maxwell Garnett (MG) model is the simplest and the most well-known model to use. This model is effectively applicable for multiphase systems.[90] The Maxwell Garnett multiphase formula for composites having particulate conducting inclusions below the percolation threshold is

$$\varepsilon_{eff} = \varepsilon_b + \frac{1}{3}\sum_{i=1}^{n} v_i(\varepsilon_i - \varepsilon_b)\sum_{k=1}^{3}\frac{\varepsilon_b}{\varepsilon_b + N_{ik}(\varepsilon_i - \varepsilon_b)}\Bigg/1 - \frac{1}{3}\sum_{i=1}^{n} v_i(\varepsilon_i - \varepsilon_b)\sum_{k=1}^{3}\frac{\varepsilon_b}{\varepsilon_b + N_{ik}(\varepsilon_i - \varepsilon_b)} \quad (9)$$

where ε_b is the relative permittivity of the dielectric matrix phase; ε_i is the relative permittivity of the i-th type of particulate inclusions; v_i is the volume fraction occupied by the conducting filler or inclusions of the i-th type; N_{ik} is the depolarization factor of the i-th type of foreign inclusions, and the indices $k = 1, 2, 3$ correspond to x, y, and z Cartesian coordinates.

In the case of composite materials assisted with the conductive inclusions around the percolation threshold, the effective permittivity can be incurred from the McLachlan's effective medium theory.[91] McLachlan's equation is suitable for tracing out the effective parameters of the mixture close to or above the percolation threshold;

$$\frac{(1 - v_i)\left(\varepsilon_b^{1/s} - \varepsilon_{eff}^{1/s}\right)}{\varepsilon_b^{1/s} + ((1 - \rho_c)\rho_c)\varepsilon_{eff}^{1/s}} + \frac{v_i\left(\varepsilon_b^{1/s} - \varepsilon_{eff}^{1/s}\right)}{\varepsilon_i^{1/t} + ((1 - \rho_c)\rho_c)\varepsilon_{eff}^{1/s}} = 0 \quad (10)$$

These above equations are derived based on the percolation threshold of the composite material. Materials with a medium range of conductivity such as polymeric materials are known as lossy materials. Where the EM wave losses its energy by heating up the medium. Pozar explained the measurement of shielding effectiveness through mathematical calculation for a lossy material like rubber composite. The equation is classified based on absorption loss and reflection loss. In the case of linear isotropic lossy materials, the alternating current (AC) electrical wave propagation has two basic components.

The free electrons/holes transport obeying the complex conductivity σ, which can be expressed as

$$\sigma = \sigma' - j\sigma'' \quad (11)$$

and the bound electron dielectric displacement implied in the permittivity which can be expressed as

$$\varepsilon = \varepsilon' - j\varepsilon'' \quad (12)$$

Where σ' and σ'' are the real and imaginary part of the complex conductivity respectively. The real component ε' is colligated to the phase of polarization and ε'' as an imaginary component is the result of the losses consorted with the dielectric damping *i.e.*, the bound electrons in the dipoles experience fluctuation of the electric field at an angular frequency designated as ω. Thus, the current density, J, determined by an electric field E, is

$$J = j\omega\left(\varepsilon' - j\varepsilon'' - j\frac{\sigma'}{\omega} + \frac{\sigma''}{\omega}\right)E \quad (13)$$

Imaginary conductivity is usually negligible at a frequency lower than 300 GHz. So, it can be assumed that

$$\sigma' = \sigma_{DC} = \sigma \quad (14)$$

Hence, we can write the current density as

$$J = j\omega\left[\varepsilon' - j\left(\varepsilon'' + \frac{\sigma}{\omega}\right)\right]E \quad (15)$$

where the term $\left(\varepsilon'' + \frac{\sigma}{\omega}\right)$ linearly depends on the total effective conductivity.

The inherent impedance of a material η is

$$\eta = \sqrt{\frac{\mu}{\varepsilon' - j(\varepsilon'' + \sigma/\omega)}} \quad (16)$$

where μ is the magnetic permeability of the composite material.

For a viscoelastic lossy material *viz.* rubbery system, the expression related to the attenuation constant α as a function of the electrical, magnetic losses and dielectric losses was reported elsewhere by Paul. The propagation constant, γ, can be expressed as

$$\gamma = j\omega\mu(\sigma + j\omega\varepsilon) \quad (17)$$

If the above equation is combined with complex permittivity we get

$$\gamma^2 = j\omega\mu\{\sigma + j\omega(\varepsilon' - j\varepsilon'')\} = j\omega\mu\{(\sigma + \omega\sigma'') + j\omega\varepsilon'\} \quad (18)$$

The propagation constant is also defined in terms of its complex components, *i.e.*, the attenuation α, and phase constant β;

$$\gamma^2 = j\omega\mu(\sigma + j\omega\varepsilon) = (\alpha + j\beta)^2 \quad (19)$$

$$(\alpha + \beta^2) + j2\alpha\beta = j\omega\mu(\sigma + \omega\varepsilon'') - \omega^2\mu\varepsilon' \quad (20)$$

Comparing from both sides

$$2\alpha\beta = \omega\mu(\sigma + \omega\varepsilon'')$$

$$(\alpha^2 - \beta^2) = -\omega^2\mu\varepsilon'$$

$$\beta = \frac{\omega\mu(\sigma + \omega\varepsilon'')}{2\alpha}$$

$$\alpha^2 - \left[\frac{\omega\mu(\sigma + \omega\varepsilon'')}{2\alpha}\right]^2 = -\omega^2\mu\varepsilon'$$

$$\alpha^2 = \frac{-\omega^2\mu\varepsilon' + \sqrt{(\omega^2\mu\varepsilon')^2 + [\omega\mu(\sigma + \omega\varepsilon'')]^2}}{2} \quad (21)$$

hence the value of α will be

$$\alpha = \omega \sqrt{\frac{\mu\varepsilon'}{2}\left[\sqrt{1+\left\{\frac{\sigma/\omega+\varepsilon''}{\varepsilon'}\right\}^2}-1\right]} \quad (22)$$

2.3 Shielding effectiveness measurement techniques

Measurement of shielding effectiveness for any composite materials, a solid material network analyser is used which is divided into two types (a) a scalar network analyser (SNA) which can compute electrical signal only, that's why it is not useful for measuring complex signals; and (b) a vector network analyser (VNA) can compute both electrical and magnetic signals and measure the transmission coefficient and reflection coefficient. Complex permeability and permittivity can be measured by analysing the reflection and transmission signals of VNA. Thus, more preference has been given to VNA as compared to the previous one.

Generally, in the case of VNA, (Fig. 2), a high frequency wave sweep to measure the signal of the EM wave ranges from a few kHz to 110 GHz or even higher is used. To measure the transmission and reflection signals of the sample, a single frequency signal launches from the source of the system to the material under test (MUT). The receiver is set to this frequency to detect the reflected and transmitted signals arising from the material. The measured response produces the magnitude and phase data at that frequency. The source is then stepped to the next frequency and the measurement is repeated to display the reflection and transmission measurement response as a function of frequency.[92]

Fig. 2 shows a schematic of the VNA technical arrangement with experimental setup. The technique involves the measurement of the reflected (S_{11}) and transmitted signal (S_{21}). The SE of the EMI shield can be expressed as

$$SE_T = 10\log_{10}\frac{1}{T} = 10\log_{10}\frac{1}{|S_{21}{}^2|} \quad (23)$$

$$SE_R = 10\log_{10}\frac{1}{1-R} = 10\log_{10}\frac{1}{1-|S_{11}{}^2|} \quad (24)$$

$$SE_A = 10\log_{10}\frac{1-R}{T} = 10\log_{10}\frac{1-|S_{11}{}^2|}{|S_{21}{}^2|} \quad (25)$$

$$A = 1 - R - T \quad (26)$$

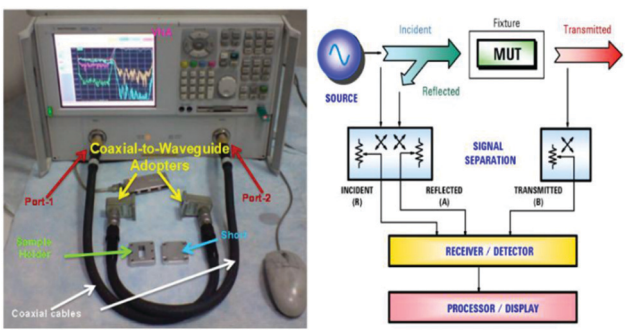

Fig. 2 Photo of two port VNA and schematic of VNA. Adapted from ref. 172 Copyright 2012, In Tech Open.

where in the above equations the *SE* provides details on the desired deactivation mechanisms whereas the coefficients give detailed information about the fractions of EM radiations lost *via* reflection as well as absorption.[93–96]

2.4 Percolation theory

The electrical conductivity of the polymer nanocomposites strongly depends on the concentration of the nanofillers,[61,62] their dispersion and distribution, processing techniques and nature of the polymer matrix.[86] In EPC's, the dispersed state of the conductive filler plays a vital role in deciding the conductivity of the composite and is well explained by the percolation theory.

The theory gives an idea about the minimal amount of conductive filler required to convert an insulating polymer matrix to a conductive one. As in Fig. 3, the conductivity *versus* filler concentration plot can be broadly divided into three regions: Region 1, 2 and 3. At a lower concentration of filler *i.e.* region 1, the composite acts as an insulating material as the filler particles are separated from one another without the formation of a continuous conductive network. Region 2 shows an abrupt increase in conductivity. In this region, a continuous conductive network forms through the arrangement of filler particles in the polymer matrix. Beyond a particular concentration, a very small increment in conductivity is observed and this particular concentration is called the electrical threshold concentration. More or less a plateau region is formed beyond the threshold concentration of filler (region 3) without any significant increase in conductivity. Excessive addition of filler above the threshold concentration can lead to an increase in agglomeration and aggregation of filler particles which will not help in improving electrical conductivity.

The percolation threshold concentration or limit can be predicted using the power law of classical percolation theory as per the equation

$$\sigma_{DC} = \sigma_o (p - p_c)^t \text{ for } p > p_c \quad (27)$$

where σ_{DC} is the DC conductivity and σ_o is a constant quantity. p and p_c are the filler fraction and filler fraction at critical or percolation concentrations respectively and t is the critical

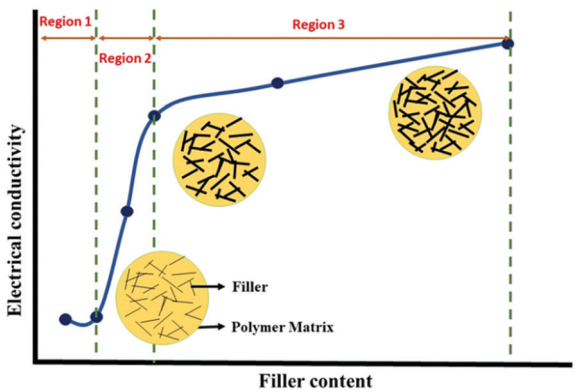

Fig. 3 Schematic diagram showing the percolation behaviour of the filler in the polymer matrix.

exponent. The critical exponent value is an important factor that indicates the lattice dimensionality of the filler.[87,88] A t value *i.e.* close to 1.5 says the electrical conductivity is due to the contact between agglomerates whose shape is close to spherical. A higher value of t (close to 3) indicates the conductivity is imparted by the contact between individual fibers.[89]

3 Preparation techniques of polymer nanocomposites

Nanocomposites are developed by the homogeneous dispersion of the nano-material (filler) in the polymeric matrix to enhance the physical properties of the composite material. The properties of a polymer nanocomposite can be modulated by varying the concentration of the nanomaterial (wt%) in the polymer matrix and using various polymerisation techniques. Various types of compounding methods are used to synthesize nanocomposites; such as (i) *in situ* polymerization, (ii) solution compounding, (iii) melt blending, (iv) sol-jet methods and (v) electro spinning. As per a literature survey, the first 3 methods are being used for synthesizing thermoplastic elastomer nanocomposites. All these methods have some pros and cons which are explained in this section.

3.1 Solution mixing

This is a solvent based method (Fig. 4). A prerequisite of this method is that the polymer should be dissolvable in the solvent such as tetrahydrofuran (THF), dimethyl formamide (DMF), toluene or acetone. Then the nanofillers are also dispersed in this polymer solvent solution. Then the solution is mixed homogenously using mechanical mixing, magnetic agitation, or high-energy sonication. Because of the high shear force the fillers are finely dispersed in the polymer matrix. Pre-dispersion of the nanofiller in the solution using ultrasonication eases mixing of the polymer and filler solution. The optimum sonication condition (power and time) can be decided based on filler concentration.[97]

As compared to other methods, here filler dispersion in the polymer matrix can be easy due to low viscosity. After mixing, the solvent is removed by evaporation and the matrix is molded to give the appropriate shape. Here, surface modification of the filler can also be done without drying. The electrical conducting composites prepared by solution compounding have a lower percolation threshold. The main disadvantage of this method is in large scale production i.e difficulties in extraction and disposal of solvent on a large scale. This is also hazardous for the environment. Several research groups have been using this method to produce thermoplastic polyurethane (TPU) based nanocomposites.

3.2 *In Situ* Polymerization

In situ polymerization takes place between a nanofiller and monomer at the beginning (Fig. 5). Covalent bonds form between the filler and polymer matrix, and because of this homogeneous dispersion strong bonding can be achieved in this method.

This method is preferred for thermally unstable or insoluble polymers which cannot be processed by other *in situ* polymerization, and is the most efficient method among the other three methods. Due to strong interaction between the filler and matrix these composites show very good mechanical properties. The main disadvantage of this technique is the consumption of a lot of electrical energy to disperse the filler in the polymer matrix, so this method is not fruitful for mass production.

3.3 Melt blending

Compared to the other two techniques melt blending is the most preferred technique for mass production (Fig. 6) because it is simple, environmentally friendly and cost effective. In this process nanofiller is dispersed into a viscous fluid of molten polymer using a high shear force. Therefore, solvents are not required and

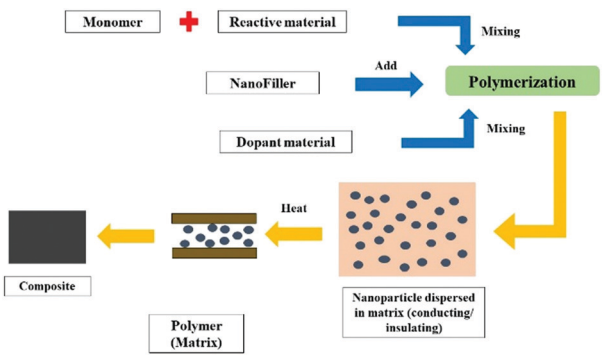

Fig. 5 The in-situ polymerization method of preparation of conductive and insulating polymers.

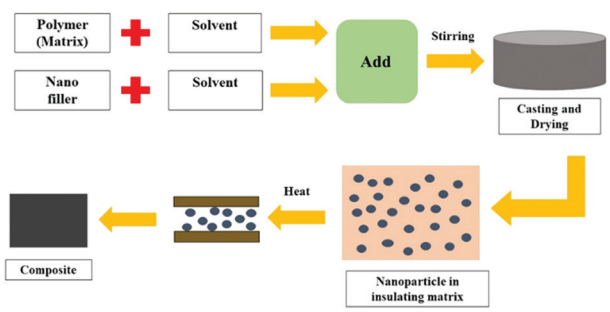

Fig. 4 Method of preparation of extrinsic polymers by solution mixing methods.

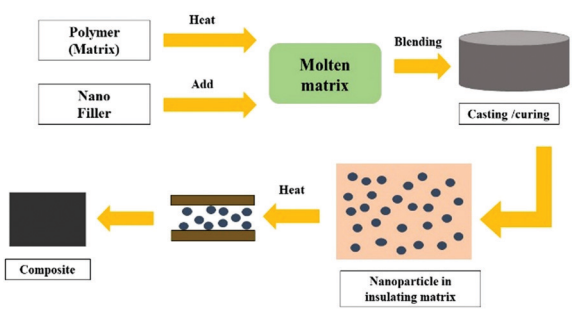

Fig. 6 Method of preparation of polymer composites by melt mixing methods.

Table 1 Polymerisation techniques of various TPE composites and their SE

Polymerisation techniques	Base polymer	Nano filler	SE (dB)	Ref.
Solution compounding	TPU	RGO (2.5%)	53	98
Solution compounding	TPU foam	RGO (3.2 vol%)	21.8	99
Solution compounding	TPU foam	Graphene	23–24	100
Melt compounding	SEBS	GNP + CNT	36.47	101
Melt compounding	SEBS	CNT	29.6	102
Melt compounding	SBS/PVDF/PVA	MWCNT		
Melt compounding	TPU	Silver	103.5	103
	Natural rubber	Fe_3O_4 reduced graphene	26.4	104

traditional mixing devices such as an extruder, internal mixer, and two-roll mill are used for these techniques.

In the case of melt blending, the percolation threshold is comparatively higher than the *in situ* polymerization or solution compounding. Unlike the studies involving *in situ* polymerisation and solution compounding techniques, here, a fine balance has often been struck between mechanical and electrical properties, which could lead to faster realization into commercial products.

Table 1 shows the compositions, shielding effectiveness (SE) and polymerisation techniques of various thermoplastic elastomer nanocomposites.

4 Thermoplastic elastomers

Thermoplastic elastomers bridge the gap between rubber and thermoplastic polymer materials. Thermoplastic elastomers possess the ability to be stretched to more than 100% strain, returning to their original shape after removal of the applied stress showing their elastomeric behaviour while ensuring the good process-ability of thermoplastics at elevated temperatures. Thus, thermoplastic elastomers are the blends which can be recycled and remoulded like thermoplastics and show the characteristic property of elastomers at ambient temperature. These blends exhibit excellent service properties at the economical price whose material properties can be modified by varying the blend component, viscosity of the components and compounding ingredients.[105,106]

The initial thermoplastic elastomer that was introduced was thermoplastic polyurethane in the 1950s.[107] Later that decade, researchers focused on the manufacturing of novel block copolymers and thermoplastic polyolefins (TPO).[108] Thermoplastic elastomers based on styrenic block copolymers became more popular in polymer industries in the 1960s.[109] The first TPE to be commercially available was a blend of partially cured mono olefin copolymer rubber with a polyolefin thermoplastic in the year 1972.[110,111] In the late 1950s, the emergence of the TPEs in the field of polymer science and technology fetched a new horizon.[112–114]

Most often the thermoplastic elastomers are block copolymers (Fig. 7) consisting of soft and mobile "rubbery" blocks with a low glass transition temperature (T_g), and rigid or hard "glassy" blocks with a high melting temperature (T_m) or high T_g. They can be commercially divided into two broad categories: (a) based on block copolymers (triblock or multi-block), and (b) based on polymer blends. The tri block copolymers have a soft and flexible

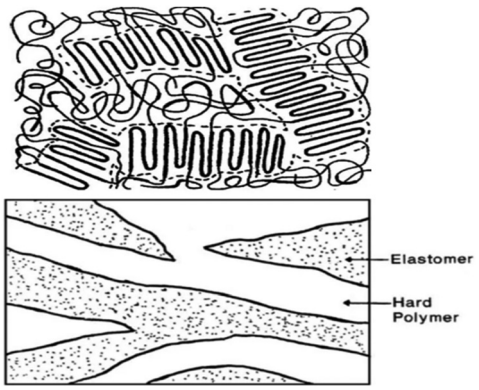

Fig. 7 Morphology of (a) a block copolymer thermoplastic elastomer and (b) a rubber/plastic blend thermoplastic elastomer (TPE). Reprinted with permission from ref. 134 copyright 2020 Elsevier Ltd.

mid-block surrounded by rigid end blocks like SBS (styrene-butadiene-styrene) or SEBS (styrene-ethylene-*co*-butyl-ene-styrene). Whereas in the multi-block copolymers, rigid or hard blocks are constituted of polyesters, polyamides or polyurethanes and polyethers form the soft blocks.[115–117]

The rigid blocks together form clusters which act as physical cross-links between the soft blocks. Under deformation, the hard blocks remain crystalline and do not deform, therefore the deformation is governed by the soft rubber domains. Under the melt temperature, the copolymer chains start to flow and the material can be processed like all thermoplastic polymers.[118–121]

Thermoplastic elastomers have various advantages like easy processability, better quality control and easy variation in properties by varying the ratio of components. They do not need vulcanization and require much less compounding. They also offer recycling of the scraps without the significant deterioration of the properties. Disadvantages of thermoplastic elastomers include creep response upon extended use and loss of elastic behaviour at a higher temperature. As the rubber phase is not cross-linked, it does not provide enough resistance to set behaviour under prolonged deformation. This led to the formation of dynamic vulcanizates or thermoplastic vulcanizates where the elastomeric phase is cross-linked leading to superior elastic behaviour.

4.1 Block copolymer based thermoplastic elastomer for EMI shielding

Various studies have reported the effectiveness of block copolymer based thermoplastic elastomers for the EMI shielding

application. Literature shows that SEBS (poly styrene-*b*-ethylene-ren-butylene-*b*-styrene) mixed with different fillers show exceptional conductivity and prove to be a suitable materials for shielding.

Kcheyla *et al.*[122] reported an electrically conductive thermoplastic elastomer composite based on the SEBS and expended graphite (EG)/carbon black (CB) through melt blending for the application of EMI shielding. They compared the electrical conductivity, as well as EMI of SEBS/EG and SEBS/CB. The incorporation of the EG and CB additives into the SEBS matrix were responsible for the composites having electrical conductivity 15 orders of magnitude higher than that of the pure SEBS. The SEBS/EG and SEBS/CB composites fabricated show high electrical conductivities of 0.2 S cm^{-1} but the SEBS/EG composites were found to have higher electrical percolation thresholds than the SEBS/CB composites. The EMI SE (Fig. 8) acceptable value for the SEBS/CB composite blended with 15 wt% of CB showed promising results for shielding applications. They showed that the electromagnetic interference shielding effectiveness increases with an increase in the additive weight fractions in the matrix. For both SEBS/EG and SEBS/CB the EMI SE was found to be predominantly due to reflection. At a higher amount of conducting additive, beyond the percolation threshold, the composite containing CB displayed a higher EMI SE than those containing a similar amount of EG.

Kuester *et al.*[102] demonstrated SEBS and carbon nanotube (SEBS/CNT) nanocomposites fabricated by melt compounding for shielding applications. The nanocomposite exhibited an EMI SE of 30.07 dB upon addition of 15 wt% of CNT in the SEBS matrix. They evaluated the electromagnetic interference shielding effectiveness (EMI-SE) of the nanocomposites for the X-band microwave frequency range which showed that maximum conductivity of approximately 1 S cm^{-1} with 8.0 wt% of CNT. EMI SE is increased with the increase in the CNT weight fraction in the prepared nanocomposite (Fig. 9 a and b). The average shielding effectiveness due to reflection, SER, is predominant at a lower weight fraction of CNT whereas the SEA contributed more at a higher CNT weight fraction for the SEBS/CNT nanocomposites.

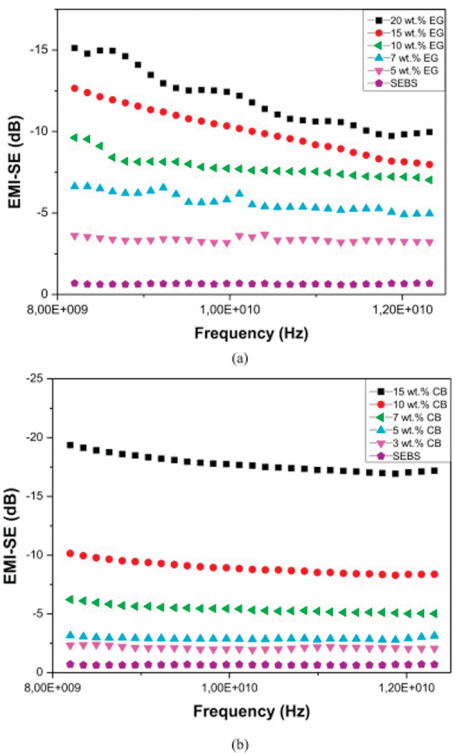

Fig. 8 EMI SE *versus* frequency for (a) SEBS/EG and (b) SEBS/CB composites with 5, 7, 10, 15 and 20 wt% of EG, and 3, 5, 7, 10, and 15 wt% of CB, respectively. Reprinted with permission from ref.122 copyright 2015 Elsevier Ltd.

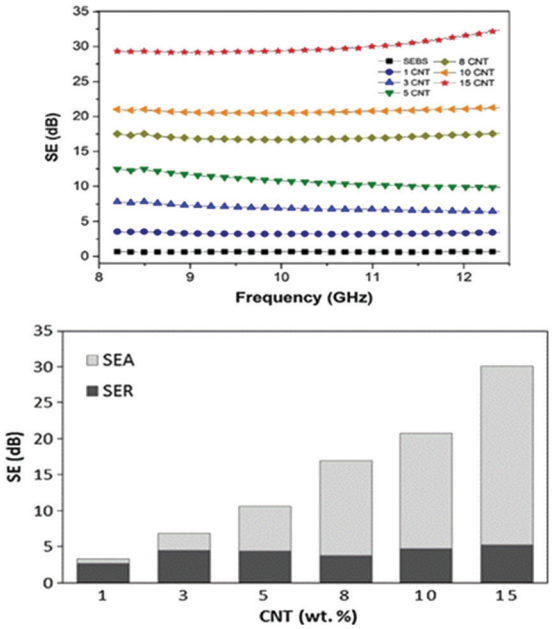

Fig. 9 (a) Shielding effectiveness *versus* frequency of SEBS/CNT nanocomposites at different CNT weight fractions. (b) Contribution of reflection (SE_R) and absorption mechanisms (SE_A) to the total EMI-SE (dB) at different CNT weight fractions for the SEBS/CNT nanocomposites. Reprinted with permission from ref. 102 copyright 2016 Elsevier Ltd.

In extension to the previous paper, Kuester *et al.*[101] reported other hybrid nanocomposites of SEBS with carbon nanotubes (CNT) and graphene nanoplatelets (GnP) fabricated by a melt mixing process and nanocomposite tested in the X band. The hybrid nanocomposites presented synergic effects on EMI-SE when compared to the single-component nanocomposites (SEBS/GnP and SEBS/CNT). The maximum EMI-SE of 36.47 dB was achieved for the SEBS/GnP/CNT nanocomposite with 5/10 wt% of GnP/CNT. The electrical conductivity increased by 17 orders of magnitude when compared to the pure polymer matrix, reaching 2/8 wt% of GnP/CNT. Fig. 10 a and b show that the EMI SE of the prepared SEBS/GnP nanocomposite increases with an increase in the weight fraction of GnP.

In their work, Xu *et al.*[123] reported reversibly cross-linked and solvent-proof SEBS/carbon hybrid composites for (EMI) shielding, utilizing Fur-SEBS as the matrix, BMI as the crosslinking agent, and FG and MWCNTs as fillers. The reaction between furan and the filler is based on the Diels Alder (DA) reaction. The composite designed was based on the microwave absorption capacity of the resulting composite which could be enhanced and a maximum SE of 36 dB was reported (Fig. 11) by the composite with 4 wt% FG and 12 wt% CNTs.

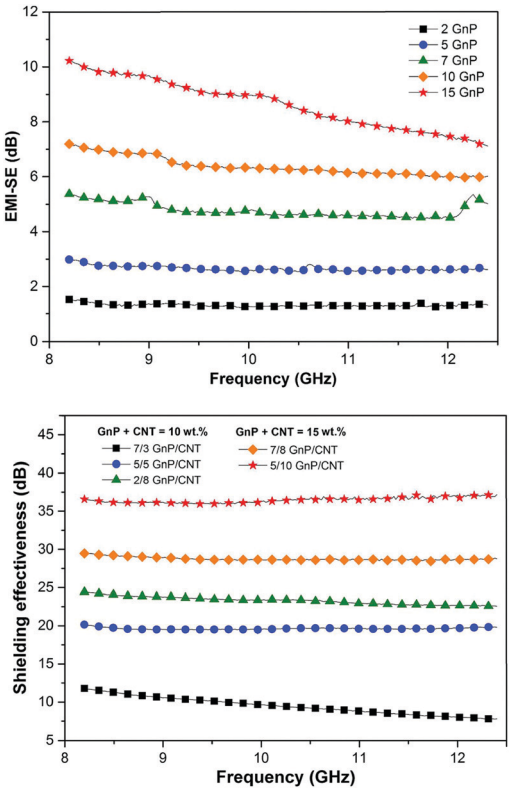

Fig. 10 (a) Shielding effectiveness of SEBS/GnP nanocomposites at different GnP weight fractions as a function of frequency. (b) Shielding effectiveness of SEBS/GnP/CNT nanocomposites at different GnP/CNT weight fractions as a function of frequency. Reprinted with the permission from ref. 101 copyright 2017 Elsevier Ltd.

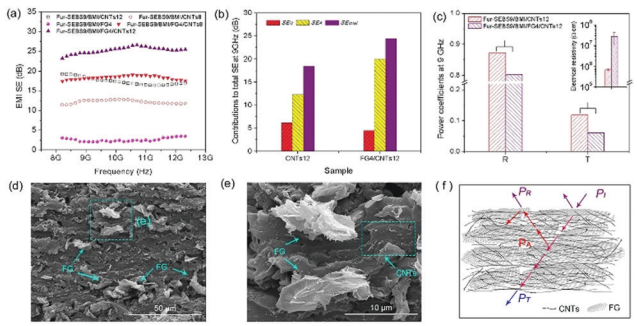

Fig. 11 EMI shielding properties of the prepared composites: (a) comparative EMI SE curves of Fur-SEBS9/BMI/FG4, Fur-SEBS9/BMI/CNTs and Fur-SEBS9/BMI/FG4/CNTs composites; (b) contribution to total SE due to absorption and reflection for Fur-SEBS9/BMI/CNTs12 and Fur-SEBS9/BMI/FG4/CNTs12 at 9 GHz; (c) power coefficients of Fur-SEBS9/BMI/CNTs12 and Fur-SEBS9/BMI/FG4/CNTs12 composites at 9 GHz; (d) SEM image of Fur-SEBS9/BMI/FG4/CNTs12; (e) magnified image of image d; (f) schematic diagram of attenuating the microwave for the Fur-SEBS9/BMI/FG/CNTs hybrid composites. Reprinted with permission from ref. 123 copyright 2018 Elsevier Ltd.

To measure the EMI SE of the novel composite material for the application of sealant and gasket in radiofrequency appliances Albers *et al.* prepared SEBS and silver nanoparticle (spheres, fibers) composites. Fiber shaped fillers exhibit more conductivity as compared to sphere shaped ones because the conductive path reduces the percolation threshold. Previously it has been studied that coating of conductive filler enhances the electrical conductivity of the composite by arresting the matrix and particle interaction and increasing inter-particle interactions. Thus, this group selected some organic solvents (ODM & DPHT) for coating. They observed that the DC conductivity and radio frequency impedance were reduced by the coating. In the case of DPHT coating, DC conduction was attained through a combination of particle alkylation and doping with polarizable π-conjugated compounds and electron tunneling was dominant in the DC conductivity of ODM coated composites. A combination of both effects was observed in the case of ODM + DPHT coated composites.[124] The RF shielding characteristics of various elastomers were evaluated in the frequency range from 20 MHz to 2000 MHz. It has been observed that in the case of RF attenuation measurements fibers gave better result as compared to the spheres and only ODM coated composites enabled an SE of 120dB, whereas the effect of DPHT was not significant.

Pan *et al.* fabricated SEBS based nanocomposite microspheres with a carbon nanoparticle (MWCNT & rGO) based filler.[125] They had prepared SEBS/MWCNT microspheres first by a solvent evaporation method. Then *in situ* reduction of graphene oxide was added to coat the SEBS/MWCNT microspheres.

Finally, segregated SEBS/MWCNT/rGO nanocomposite microspheres were achieved by hot pressing, as shown in Fig. 12, for further study such as electrical conductivity, percolation threshold, and EMI SE were done on the sample.

This group observed that a conductive 3-D network was formed in the SEBS/MWCNT/rGO composite where rGO was the most important for the conductive path. Though MWCNT had little effect on the conductive network, it does not affect the percolation threshold of the composite because MWCNT is covered by an insulated SEBS matrix. When the SEBS matrix was loaded with 2.1 vol% CNT and 3.3 vol% rGO, the conductivity reaches 0.14 S/m, which is 16 orders of magnitude greater than the original SEBS matrix. It is found that the composite samples have an excellent EMI shielding performance due to their special 3D conductive network. The EMI SE of the composite filled with 2.1 vol% CNT and 3.35 vol% rGO

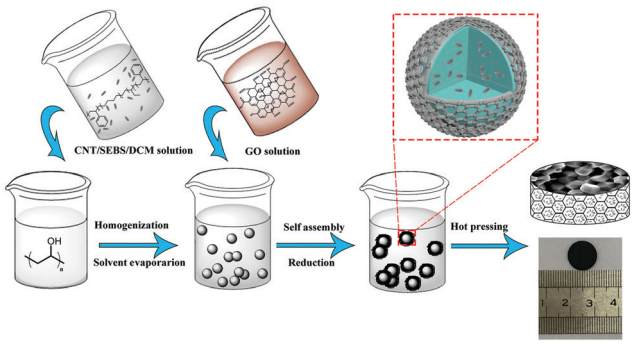

Fig. 12 Schematic of the preparation of SEBS/MWCNT/rGO nanocomposite microspheres. Reprinted with permission from ref. 125 copyright 2019 Wiley Periodicals, Inc.

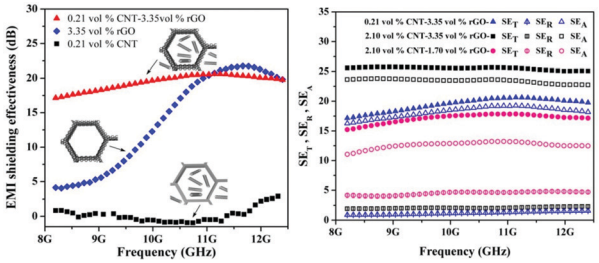

Fig. 13 Influence of CNT/rGO filler ratio on the EMI SE of the CNT/SEBS/rGO nanocomposite in X band frequency. (a) EMI SE of the composite filled with a different single filler, and (b) SE contribution in the composite at 3 different sample mixtures. Reprinted with permission from ref.125 copyright 2019 Wiley Periodicals, Inc.

reaches 26 dB in the X band (meaning that 99.75% of the incident EM radiation is blocked) as shown in Fig. 13, which is 6 dB higher than the commercial requirement of 20 dB. From the perspective of EM energy distribution analysis, its reflectance coefficient (19–41%) reveals that the main shielding mechanism is absorption. On the basis of contrast experiments, the results show that the EM absorption ability is greatly influenced by the content of CNT and rGO, molding temperature.[125]

Another EMI shielding material based on SEBS was reported by Zhao *et al.*[126] which is based on ZrO_2-coated graphene oxide (GO)/SEBS. These nanocomposites showed an excellent EMI shielding effectiveness (SE) of 37.9 dB (Fig. 14) over the X band. The SEBS/ZrO_2-coated GO nanocomposite showed better oxidation resistance due to a high-order architecture and effective compatibility due to better interaction between the ZrO_2-coated GO and SEBS matrix surfaces.

Styrene-butadiene-styrene copolymer (SBS) based composites have also been proved to have excellent EMI shielding properties. A conductive (SBS/CNT) composite foam with three-dimensional networks, reported by Tian *et al.*[127] was made by freeze-drying technology. The SBS copolymer helped strengthen the CNT framework and improved the mechanical strength of the composite foam. With a loading of 9 wt% CNTs, the composite foam exhibited an excellent compression modulus of 1.15 MPa and good recovery of 32%. Furthermore, it also showed an outstanding total EMI shielding effectiveness above 47 dB within the frequency scope of 8.4–12.4 GHz and electrical conductivity of 51.8 S m^{-1}.

4.2 Thermoplastic PEBA based thermoplastic elastomer composite for EMI shielding

Thermoplastic elastomer poly ether block amide (PEBA) is a block copolymer composed of rigid polyamide (PA6, PA11, PA12) and flexible alcohol terminated polyether (PEG) by condensation reaction. These polymers exhibit low density and good flexibility under varying temperature with high strength and toughness.[128] PEBA resin has a high gas permeability, which can help the sorption of a foaming agent and reduce the required foaming time.[129] It can be easily dissolved in the environmentally friendly solvent ethanol.[130] PEBA resin can be synthesized from biomass raw materials, and it can be recycled by simple eco-friendly methods.[131]

Wang *et al.* prepared flexible and conductive PEBA/MWCNT nanocomposite films in solid and porous (microcellular and nanocellular) structures. Microcellular, co-microcellular and nanocellular foaming was created by biaxial stretching with ε = 0.5, ε = 1 and ε = 1.5. The presence of MWCNT and biaxial stretching refined the cellular structure and give uniformity. Solid PEBA/MWCNT nanocomposite films exhibit a conductive nature due to the MWCNT nanoparticles which create a conductive network in the PEBA matrix. But the conductivity properties decrease in the case of microcellular foaming because the micro cell is too large compared to the particle size MWCNTs, which could muddle the conductive network. In the case of nanocellular PEBA/MWCNT, the conductivity increased two orders of magnitude higher than the solid sample (Fig. 15).

In this case MWCNT reorientation increases the contact opportunity of MWCNTs, thereby increasing the conductive networks and improving conductivity. For EMI shielding

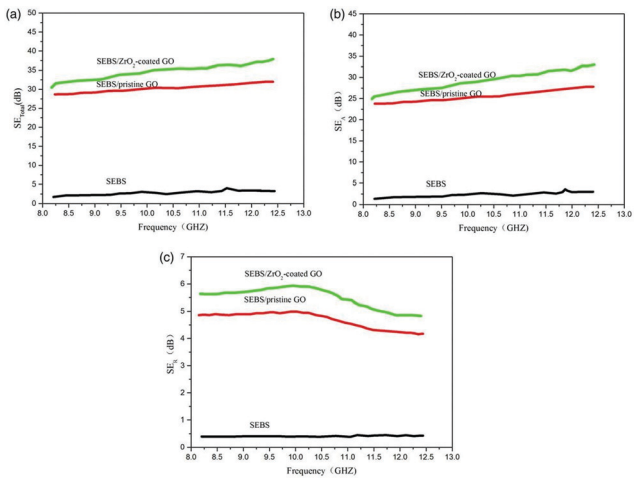

Fig. 14 EMI SE of SEBS/pristine GO and SEBS/ZrO_2-coated GO over the X-band (a) SET; (b)SE_A; and (c) SE_R. Reprinted with permission from ref. 126 copyright 2018 Society of Plastics Engineers.

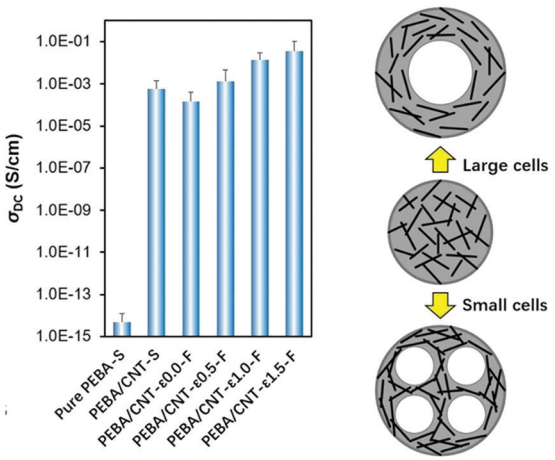

Fig. 15 DC conductivity of solid and foamed PEBA and PEBA/MWCNT composites (left) and a schematic illustration of the effect of cell growth on fiber orientation and distribution (right). Adapted from ref. 132 copyright 2021 The Royal Society of Chemistry.

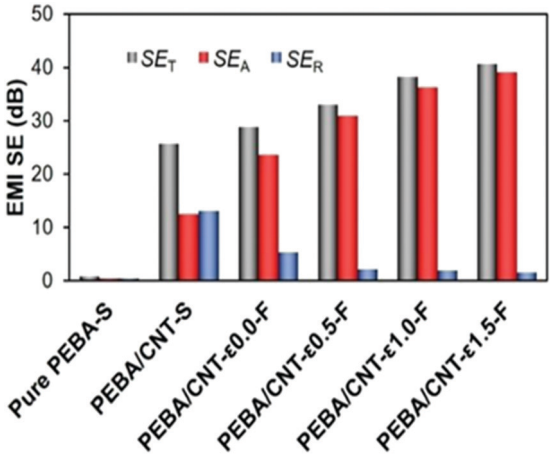

Fig. 16 The EMI SE behaviour of solid and porous PEBA/MWCNT nanocomposite films with their contribution by reflection, absorption and multiple reflection. Adapted from ref. 132 copyright 2021 The Royal Society of Chemistry.

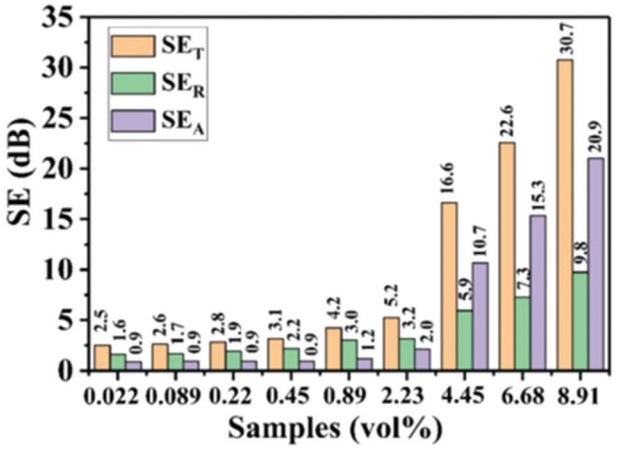

Fig. 17 Graphical comparison of average total shielding (SE_T), reflection (SE_R) and absorption (SE_A) of PEBAX/graphene composite films of various volume%. Adapted from ref. 133 copyright 2020 The Royal Society of Chemistry.

properties both solid and porous PEBA/MWCNT nanocomposite films exhibit outstanding behaviour. Porous films have an enhanced EMI shielding capacity compared with solid films. Reducing cell size leads to enhanced EMI shielding performance. While the solid PEBA/MWCNT nanocomposite film shows a SET value of 26 dB, the nanocellular PEBA/MWCNT nanocomposite film possesses a SET value as high as 41 dB. (Fig. 16) More importantly, the nanocellular PEBA/MWCNT nanocomposite film shows an absorption-dominated EMI shielding behaviour, while the solid one shows a reflection-dominated EMI shielding behaviour.[132]

Chengbiao *et al.* made a microcellular PEBA/MWCNT composite by preparing PEBA foam bead and PEBA + MWCNT solution separately and mixed all of them for uniform distribution. A segregated composite was achieved by using pressure on the mixture. In this composite good conductivity and EMI shielding effectiveness was achieved due to the segregated structure and excellent flexibility and hysteresis was about 15% during cyclic tension and compression deformation was achieved because of the PEBA matrix. This group also observed that the conductivity and EMI shielding properties of these composites did not vary from the initial value, under the application of multiple deformation in the tension and compression mode.[131]

Zhao *et al.* prepared a PEBA/graphene nanocomposite film using a facile melt mixing scheme and varying the concentration of filler from 0 to 8.9 vol%.[133] They observed the effect of graphene concentration on the electrical, mechanical and EMI shielding properties of the film. The film was flexible up to the concentration of 4.45 vol%. With the increment of graphene loading the electrical conductivity and EMI shielding properties enhanced. EMI shielding reaches up to 30.7 dB (Fig. 17) and the shielding mechanism of the material preferred more absorption than reflection. Their prime focus was to observe the electrical behaviour with the application of pressure. The composite film exhibits a linearly negative pressure effect with more conductivity. The composite films show good sensitivity, recoverability and reproducibility after stabilization by cyclic pressure loading, and also possess good discernment in pressure sensing.[133]

4.3 Polyolefinic based nanocomposite

Polyolefin thermoplastic elastomers are the materials combining polyolefin semi-crystalline thermoplastic and amorphous elastomeric components. They exhibit rubber-like characteristics and can be processed as melts by common thermoplastic processing equipment. Polyolefin nanocomposites based on nanofillers offer opportunities for the improvement of polyolefins (POs) with relatively small amounts of nanofiller concentration. Polyolefins became popular due to their low cost, recyclability, good processability, non-toxicity and biocompatibility. POs have a wide range of applications in orthopaedic implants, durable equipment automobile parts, consumer goods and industrial machinery.[134]

Park *et al.* prepared poly(ethylene-*ter*-1-hexene-ter-divinylbenzene) terpolymer (PEHV) and graphene nanocomposites by a solution casting method. The mechanical properties improved slightly with the addition of graphene. Though the EMI shielding behaviour of the material has not been observed by the group they have predicted the possibility of application in this field because of the electrical properties. The electrical resistance was decreased and capacitance was increased with the addition of graphene filler even if the amount was small.[135] iPP/MWCNT is a continuous phase such that the MWCNTs are properly dispersed in the iPP phase to form a more conductive network. Percolation theory shows the 3-D and 2-D conductive network in the segregated and conventional sample respectively. As a result the segregated sample will have a high conductivity and low percolation threshold as compared to the conventional sample. The average EMI SE of the segregated sample is more than the conventional sample at same concentration of MWCNTs because of the continuous and dense distribution of MWCNT networks and higher interfacial reflection between the iPP and POE phase. Furthermore, the segregated samples

also exhibited a relatively linear negative temperature coefficient (NTC) effect through wide temperature ranges of 45–120 °C and 150–190 °C because of the anisotropic volume expansion effect caused by the segregated structure.[136]

4.5 Thermoplastic polyurethane based thermoplastic elastomer composites for EMI shielding

Thermoplastic materials are commonly the matrix of conductive polymer composites, such as polypropylene (PP),[137] polyethylene (PE),[138] polymethyl methacrylate (PMMA),[139] poly-styrene (PS),[140] and poly(vinylidene fluoride) (PVDF).[141] Although these composite materials have a high mechanical strength and electromagnetic shielding effect, they generally have low flexibility and elasticity, leading to limited applications. Therefore, the thermoplastic elastomer is a strong candidate for preparing flexible conductive composites. Thermoplastic polyurethane (TPU), one of the thermoplastic elastomers, has attracted widespread attention due to its excellent properties such as high modulus, high strength, excellent wear resistance, chemical resistance, and low temperature resistance.[142] Therefore, TPU is widely used in a variety of industries, such as cable, automotive, medical, heavy engineering, construction and sports, and its application scope can be further expanded by introducing inorganic conductive additives.[143]

Valentini *et al.*[144] fabricated a TPU composite with EG (0 to 20 wt%). The TPU composite sample with 4 mm thickness and 20 wt% of EG exhibited excellent shielding effectiveness with an average value of −20 dB in the X band frequency range. A flexible and lightweight thermoplastic polyurethane/reduced graphene oxide (TPU/RGO) composite foam was reported by Jiang *et al.*[99] which was prepared using a supercritical CO_2 foaming method. With the increase in RGO content, the electrical conductivity and EMI shielding of the samples increased because of the improvement in the conductive network. For solid samples, an electrical conductivity of 2.77 S/m and an EMI SE of 24.7 dB were achieved with only 3.71 vol% RGO loading when tested in the X-band. Jun *et al.*[145] fabricated graphene nanoribbon (GNR)/TPU and MWCNT/TPU composites. They reported a shielding effectiveness of 24.9 dB for GNR/TPU which was significantly greater than that of the MWCNT/TPU composite (9.3 dB) achieved at 8.2 wt% with enhanced contribution from absorption. The GNR/TPU composite exhibited a significantly enhanced electrical conductivity of 1.9×10^{-4} S cm^{-1}, three orders of magnitude higher than that of the MWCNT/TPU composite (1.1×10^{-7} S cm^{-1}).

Li *et al.*[146] prepared a flexible thermoplastic polyurethane (TPU) with flake-shaped nano graphite polymer composite membranes with enhanced mechanical and EMI shielding properties. The EMI shielding effect of the TPU/G composites increased with the increase in graphite content (Fig. 18a). However, the EMI shielding effect of the TPU/GF composite decreased in contrast to the corresponding TPU/G composite, as shown in Fig. 18b. This phenomenon was predicted to be a result of breakdown in the conductive network generated by graphite flakes. It is commonly known that foaming within limits can contribute to the improvement of the conductivity as well as the EMI shielding. When the foam expansion ratio is larger than a critical value, it will be difficult to generate conductive networks, as shown by the increased percolation threshold, due to its high orientation of conductive additive.

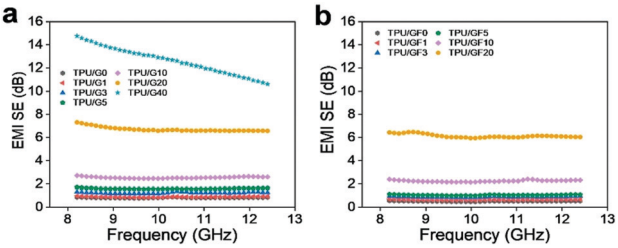

Fig. 18 EMI shielding performance of (a) solid and (b) foamed samples. Reprinted with permission from ref.146 copyright 2020 Elsevier Ltd.

Another group, Shen *et al.*,[147] reported strong flexible polymer/graphene composite films for ideal electromagnetic interference (EMI) shielding applications with a sandwich structure consisting of polyester non-woven fabric as a reinforcing interlayer and thermoplastic polyurethane (TPU) and graphene loading as a conductive coating layer. The fabricated film composite with a graphene loading of 20% exhibited a qualified bandwidth of shielding effectiveness (SE) $\geq$ 20 dB as wide as ~49.1 GHz in a broadband frequency range of 5.4–59.6 GHz. Esfahani *et al.*[148] prepared nanocomposites based on TPU and both unmodified and surface functionalized graphene sheets *via* a solution mixing process. The influence of graphene modification on the electrical and dielectric properties were studied for both groups of composites loaded with various levels of filler. The study showed that the TPU/mTRGO composites exhibited a higher electrical conductivity and improved dielectric properties due to the stronger interfacial interaction between the mTRGO and the TPU matrix. The TPU/mTRGO film with 5 vol% graphene and thickness of 1 mm exhibited commercially relevant EMI SE of ~25 dB in the X-band frequency range.

Hong *et al.*[149] fabricated the aligned Fe_3O_4@RGO/TPU composites, random Fe_3O_4@RGO/TPU and random RGO/TPU composites. The random Fe_3O_4@RGO/TPU composites showed 224% increased EMI SE over random RGO/TPU composites. The highest EMI SE, a 250% improvement over random RGO/TPU composites, was observed in the in-plane aligned Fe_3O_4@RGO composite among the four different composites. The orientation of fillers can play a key role in determining the EMI SE in the composites (Fig. 19).

Ji *et al.*[150] demonstrated a thermoplastic polyurethane (TPU) based composite with a carbon nanotube (CNT) conductive filler and intumescent flame retardants TPU/IFR/CNT by a melt compounding process. The results showed that the addition of 1 wt% CNTs and 10 wt% IFRs into TPU could achieve good flame retarding and electromagnetic interference (EMI) shielding properties simultaneously. On the other side, the particle compounding was also beneficial for improving the dispersion of CNTs and establishing the continuous conductive pathways among the IFR particles. As a result, the TPU/IFR/CNT system obtained a higher conductivity than that of the TPU/CNT system and its EMI SE even reached 20 dB, which was sufficient to meet

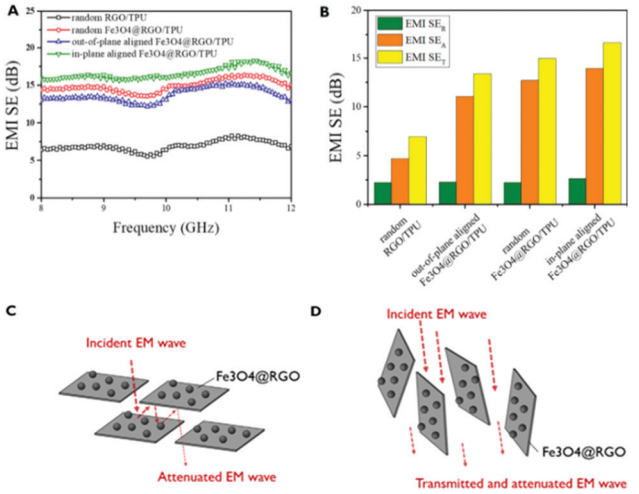

Fig. 19 EMI shielding effectiveness results as a function of frequency measured in the 8–12 GHz range (X-band) of the RGO/TPU and Fe_3O_4@RGO/TPU composites with three different Fe_3O_4@RGO orientations: random, out-of-plane, and in-plane (A). Total EMI SE (SE_T) of the RGO/TPU and three different Fe_3O_4@RGO/TPU, and their EMI SE reflection (SE_R) and EMI absorption (SE_A) (B). EMI SE schematic description of the EMI shielding mechanism of Fe_3O_4@RGO aligned TPU; in-plane direction (C) and out-of-plane direction (D). Reprinted with permission from ref.149 copyright 2020 Elsevier Ltd.

the practical requirements of many electronic devices. In another work Ji *et al.*[151] reported a multi layered TPU-based composite consisting of flame-retarding and conducting layers fabricated *via* layer-multiplying co extrusion. The average EMI SE of 32.7 dB in the X band was obtained with less than 4 wt% CNTs, exhibiting a competitive advantage in comparison to the composites made by conventional methods. By virtue of the appropriate layer space and the addition of CNTs, the V-0 rating and low heat release were achieved with the production of continuous and foaming chars in the combustion. Moreover, the average SE value of the char residue was even beyond 60 dB, demonstrating that the material could also fulfill excellent EMI shielding after experiencing a complete burning process. Therefore, the present strategy paved a new way to fabricate EMI-shielding composites with comprehensive performances. In this research work Fu *et al.*[152] fabricated an excellent and lightweight TPU-GNSs@MF composite. The resultant TPU-GNSs@MF composite with 3D porous structure had a high electrical conductivity of 45.2 S m^{-1} and an exceptional shielding effectiveness (EMI SE) of 35.6 dB in the X-band at only 2.01 vol% GNSs loading and 2 mm thickness of TPU-GNSs@MF composites. More importantly, an extraordinary EMI shielding performance durability was demonstrated in the obtained TPU-GNSs@MF even undergoing vigorous physical and chemical damage and long-term compression cycles. The compressible and robust TPU- GNSs@MF with efficient EMI shielding performance will be potentially suitable for the next-generation of flexible and portable electronic devices.

In their research work, Shin *et al.*[153] reported light weight and flexible TPU based composite films with different lengths of CNTs for superior EMI shielding efficiency and thermal management performances. Herein, the effect of different lengths of CNTs on the EMI shielding, electrical and thermal conductivity performance of TPU nanocomposites have been studied explicitly. The composite with long length CNT (10 wt%) offered a remarkable EMI shielding efficiency of 42.5 dB and electrical conductivity of 1.9×10^{-3} S cm^{-1}, whereas the composite with short length CNTs showed a thermal conductivity of 0.51 W m^{-1} K^{-1} and the corresponding thermal conductivity enhancement efficiency exceeded 145% relative to pure TPU. The composites showed a high response in electrical conductivity and minor change in EMI shielding efficiency with repeated bending cycles.

Jiang *et al.*[154] fabricated TPU/GA composite foams through the vacuum assisted impregnation method using the GA as the template followed by $scCO_2$ foaming, during which multi-stage networks were formed. The TPU/GA composite foams displayed good electrical conductivity and EMI shielding performance. The electrical conductivity of the TPU/GA composite foam was 50 S m^{-1} and the EMI shielding value was 34.3 dB with 2 wt% GA. And the introduction of the cellular structure of TPU provided the EMI waves with more paths, resulting in the improvement of the EMI shielding absorption coefficient A and the reduction of the EMI shielding reflection coefficient R. Bansala *et al.*[155] fabricated thermoplastic polyurethane (TPU)-based nanocomposites with different concentrations (ranging between 0 and 5.5 vol%) of TRG nanosheets for the application of EMI shielding. The fabricated nanocomposite showed an excellent shielding effectiveness of between −26 and −32 dB in the Ku band frequency region. Results obtained in this study clearly demonstrate that TPU/TRG nanocomposites are potential novel materials that can be utilized for protection against electromagnetic pollution. In similar research work, Bansala *et al.*[156] prepared thermoplastic polyurethane (TPU) based nanocomposite films with chemically reduced graphene (CRG) and thermally reduced/annealed graphene (TRG). The EMI shielding effectiveness for neat CRG and TRG graphene sheets was reported (Fig. 20) to be −80, −45 dB, respectively, at 2 mm thickness in the Ku band. The EMI shielding data revealed that TRG/TPU nanocomposites showed better shielding at a lower concentration (10 wt%), while CRG displayed better attenuation at higher concentrations.

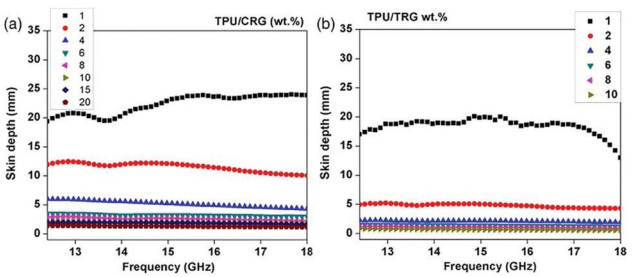

Fig. 20 Variation of skin depth with frequency of the (a) TPU/CRG and (b) TPU/TRG nanocomposites. Reprinted with permission from ref. 156 copyright 2019 Wiley Periodicals, Inc.

Verma *et al.*[157] designed nanocomposite materials based on commercial thermoplastic polyurethane filled with graphene, which are new alternative candidates for electrostatic charge dissipation and electromagnetic interference shielding applications due to their light weight, ease of processing and tunable electrical conductivities. The solution blending approach was used to fabricate a series of polyurethane/graphene (PUG) nanocomposites with graphene loading ranging from 0–5.5 vol%. The shielding effectiveness of −21 was achieved in the frequency range of 8.2–12.4 GHz (X band) at 5.5 vol% graphene loading.

Feng *et al.*[158] reported the use of microwave selective sintering to prepare mechanically strong segregated TPU/CNT composites for the EMI shielding. The obtained microwave sintering TPU/CNT composites with 5.0 wt% CNTs showed an excellent conductivity and an EMI SE of 17.9 S m^{-1} and 35.3 dB, respectively. In their research, Durmus *et al.*[159] prepared a flexible TPU–CNF–Fe_3O_4 nanocomposite having the composition of 80–5–15 wt% showing the reflection loss (RL) value of −32 dB which signified that the composite material could absorb the 97% of an incident electromagnetic wave at around 12.14 GHz. Gulzar *et al.*[160] presented nanocomposites composed of cobalt ferrite ($CoFe_2O_4$), thermoplastic polyurethane (TPU), and fly ash. They focused on the change in electrical conductivity due to increasing the concentrations of fly ash and cobalt ferrite. The highest EMI shielding of 35 dB was reported within a vast range of frequencies from 0.1 to 8 GHz. Jan *et al.*[161] reported that liquid-exfoliated, high-aspect-ratio, few-layer a33 are utilized as a filler in TPU for EMI shielding applications in the X-band (8–12 GHz). GNS–TPU composites are fabricated *via* the solution processing technique. Free-standing composite films are turned conducting from insulating as the GNS content is increased. For the TPU only film, the EMI shielding effectiveness value is about 1 dB. At maximum loading (0.12 Vf GNS), the EMI shielding effectiveness of about 14 dB is attained in the X-band. In another work, Jan *et al.*[162] theoretically estimated the EM shielding effectiveness of GNS-TPU composites both as a function of concentration and temperatures. Dielectric characteristics, measured experimentally (25 kHz–5 MHz) are particularly utilized for the theoretical evaluation. The percolative network formation at 0.0055 Vf GNS-TPU composites was further enhanced at higher temperatures as the electrical conductivity was increased and thus the EMI shielding effectiveness. A total shielding effectiveness of ∼139 dB is predicted at 473 K, making these composites a suitable candidate for such applications.

Kasgoz *et al.*[163] studied the effect of processing method on microstructure formation and the related electrical conductivity and electromagnetic interference shielding effectiveness of carbon nanofiber (CNF) filled thermoplastic polyurethane (TPU) composites. They prepared the composite *via* three different processing techniques; melt compounding (MC) in a twin-screw extruder, simple solution mixing (SM) on a magnetic stirrer, and solution mixing with sonication (SM-U). They found that SET values of samples including 20 phr of CNF prepared with MC, SM-U and SM methods varied in the range of 10–30 dB, 20–60 dB and 20–80 dB, respectively within a frequency range of 1–12 GHz. Ramôa *et al.*[164] prepared an electrically conducting thermoplastic elastomer composite based on thermoplastic polyurethane (TPU) and carbon nanotubes (CNTs) through melt blending. The study focused on the electrical conductivity, morphology, rheological properties and electromagnetic interference shielding effectiveness (EMI SE) of the TPU/CNT composites and compared them with those of carbon black (CB)-filled TPU composites prepared under the same processing conditions. EMI SE and electrical conductivity was found to be increased with an increasing amount of conductive filler, due to the formation of conductive pathways in the TPU matrix. EMI SE values found for TPU/CNT and TPU/CB composites containing 10 and 15 wt% conductive fillers, respectively, were in the range −22 to −20 dB, indicating that these composites are promising candidates for shielding applications. Zahid *et al.*[98] fabricated nanocomposites based on TPU and reduced graphene oxide (RGO) and evaluated their shielding properties in a microwave range (11 GHz to 20 GHz) as well as near infrared (NIR) wavelength range (700–2500 nm). The maximum shielding effectiveness obtained was 53 dB with the addition of 2.5% RGO. The increase in shielding effectiveness was mainly achieved in the frequency range of 12–14 GHz. Transmission observed in the IR region was less than 0.5%. The nature of the filler, the interaction of the filler with the polymer matrix and the dispersion state primarily contribute in increasing the EMI SE.

4.6 Rubber/plastic blend based thermoplastic elastomer composite for EMI shielding applications

Thermoplastic vulcanizates (TPVs) mainly based on ethylene-propylene-diene rubber (EPDM) and polypropylene (PP) have been extensively used in many industries. These kinds of materials behave like a thermoplastic polymer despite having cross-linked droplets of rubber which result in properties of rubbery materials at room temperatures such as good processability, high impact resistance, and recyclability.[165,166] For the preparation of the conductive nanocomposite, carbon nanoparticle-like carbon nanotubes (CNTs) are used.[167] Comparing TPVs to TPE composites prepared by a similar processing method, TPVs show an enhanced electromagnetic interference (EMI) performance and balanced mechanical performance at a lower percolation threshold.

Mehranvari *et al.*[168] fabricated an electrically conductive thermoplastic elastomer nanocomposite based on PP/EPDM (40/60 wt%) and MWCNT as a conductive filler by dynamic vulcanization. The EMI shielding and the complex permittivity of the sample tested in the X-band frequency. The EMI shielding result revealed that in all the samples, absorption had a major contribution in shielding effectiveness. The EMI shielding effectiveness increased upon increasing the CNT filler percentage in the nanocomposite.

A flexible composite (PP/EPDM/NCGF) for EMI shielding consisting of NCFG (nickel coated glass fiber) as a conductive filler and PP/EPDM as a matrix was prepared by electroless deposition and melt reactive process demonstrated by Duan *et al.*[169] The composite with 0.789 vol% Ni of filler showed conductivity of 0.42 S m^{-1} and SE of 22.2 dB in the X-band.

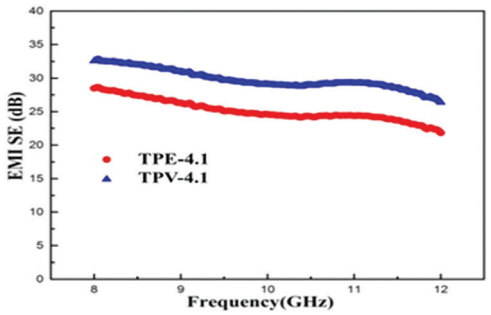

Fig. 21 EMI SE for TPE-4.1 and TPV-4.1 composites as a function of frequency in the X-band. Reprinted with permission from ref.170 copyright 2020 Elsevier Ltd.

Adding 1 vol% Ni (16.36 vol% NCGF) gave an elongation at break of 126.5%. The obtained EMI shielding effectiveness and mechanical property suggested that TPV/NCGF is a favourable lightweight, recyclable and low cost shielding material.

Ma *et al.*[170] (Fig. 21) also fabricated a flexible and lightweight composite for EMI shielding in which MWCNTs were used as the filler and PP/EPDM (50/50) as a matrix by a melt mixing method. The prepared TPV composite exhibited (Fig. 21) a good EMI SE of 28 dB at 4.1% loading of MWCNT in the X-band. The composite with PP/EPDM (50 : 50 wt%) showed little increase in gauge factor (GF) at 100% strain loading, showing excellent potential to be used as a highly stretchable conductor material.

Sharika *et al.*[171] fabricated a conductive nanocomposite with PP/NR as matrix MWCNTs with different loading (1, 3, 5 and 7 wt%) by a melt mixing method with a tunable EMI SE. The work focused on the effects of phase morphology and selective distribution of the filler in the NR phase on the EMI performance of the materials. Both system PP/NR (80/20) and PP/NR (50/50) with 7 wt% MWCNT exhibit (Fig. 22 and 23) a total SE of around 20 dB at 3 GHz.

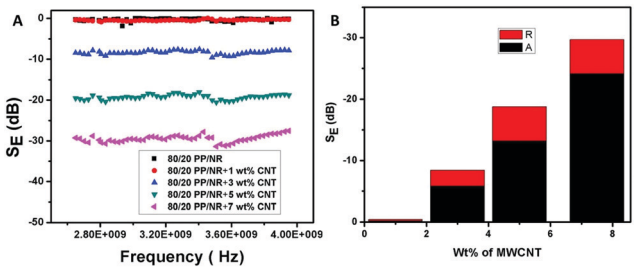

Fig. 22 (a) Total shielding effectiveness as a function of frequency for 80/20 PP/NR blend composites. (b) Contribution of reflection and absorption losses to shielding effectiveness of composites with MWCNT at 3 GHz. Reprinted with permission from ref. 171 copyright 2019 Elsevier Ltd.

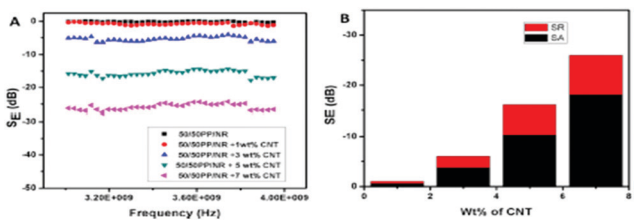

Fig. 23 (a) Total shielding effectiveness as a function of frequency for 50/50 PP/NR blend composites. (b) Contribution of reflection and absorption losses to shielding effectiveness of composites with MWCNT at 3 GHz. Reprinted with permission from ref.171, 2019 Elsevier Ltd.

5 Conclusions

In this article we have highlighted the recent research progress in the development of thermoplastic elastomers with a conductive filler like carbon black, CNT, MWCNT and hybrid fillers for EMI shielding applications. A concise introduction to EMI shielding has been reviewed. Then, thermoplastic elastomer materials with various methods and strategies to develop high-performance, light weight and cost-effective carbon filler reinforced thermoplastic elastomer polymer composites for EMI shielding applications have been summarized in detail. A lot of research has been done on conductive thermoplastic, non-conductive thermoplastic materials with conductive filler and elastomer materials with conductive filler for EMI shielding applications. Most of the composites based on elastomer and conductive filler are mostly flexible materials for EMI shielding applications. But these elastomer composites need a high conductive filler and curing process. Therefore, TPEs and carbon nanoparticle composite materials could be new highly-flexible, high-performance materials for EMI shielding applications.

Author contributions

A. K. conceived the review framework, writing, and structured the figures accordingly. J. N. carried out the review and edit. N. C. D. supervised, reviewed and edited, and acquired the funding. All authors discussed and commented on the work during the drafting of the manuscript.

Conflicts of interest

There are no conflicts to declare.

Acknowledgements

Narayan Chandra Das gives thanks to SERB, Government of India (CRG/2021/003146) for funding this research work.

Notes and references

1 D. D. L. Chung, Electromagnetic interference shielding effectiveness of carbon materials, *Carbon*, 2001, **39**(2), 279–285.
2 D. Markham, Shielding: quantifying the shielding requirements for portable electronic design and providing new solutions by using a combination of materials and design, *Mater. Des.*, 1999, **21**(1), 45–50.
3 M. Gurusiddesh, B. J. Madhu and G. J. Shankaramurthy, Structural, dielectric, magnetic and electromagnetic interference shielding investigations of polyaniline decorated

Co 0.5 Ni 0.5 Fe_2O_4 nanoferrites, *J. Mater. Sci.: Mater. Electron.*, 2018, **29**(4), 3502–3509.

4 Z. H. Shen Gong, M. Zhu, U. Arjmand, J. T. W. Y. Sundararaj and W. Zheng, Effect of carbon nanotubes on electromagnetic interference shielding of carbon fiber reinforced polymer composites, *Polym. Compos.*, 2018, **39**(S2), E655–E663.

5 D. D. L. Chung, Carbon materials for structural self-sensing, electromagnetic shielding and thermal interfacing, *Carbon*, 2012, **50**(9), 3342–3353.

6 N. C. Das, T. K. Chaki and D. Khastgir, Effect of filler treatment and crosslinking on mechanical and dynamic mechanical properties and electrical conductivity of carbon black-filled ethylene–vinyl acetate copolymer composites, *J. Appl. Polym. Sci.*, 2003, **90**(8), 2073–2082.

7 L. Kheifets, A. A. Afifi and R. Shimkhada, Public health impact of extremely low-frequency electromagnetic fields, *Environ. Health Perspect.*, 2006, **114**(10), 1532–1537.

8 R. Matthes, J. H. Bernhardt and A. F. McKinlay, International Commission on Non-Ionizing Radiation Protection. ICNIRP statement on the ''Guidelines for limiting exposure to time-varying electric, magnetic, and electromagnetic fields (up to 300 GHz)'', *Health Phys.*, 1998, **74**(4), 494–522.

9 E. Cardis, Brain tumour risk in relation to mobile telephone use: Results of the INTERPHONE international case-control study, *Int. J. Mol. Epidemiol.*, 2010, **39**, 675–694.

10 P. Parajuli, J. P. Panday, R. P. Koirala and B. R. Shah, Study of the Electromagnetic Field Radiated from the Cell Phone Towers Within Kathmandu Valley, *Int. J. Appl. Sci. Biotechnol.*, 2015, **3**(2), 179–187.

11 R. Matthes, J. H. Bernhardt and A. F. Mckinlay, Guidelines on limiting exposure to non-ionizing radiation, *ICNIRP*, 1999, **7**, 99.

12 J. Joo and A. J. Epstein, Electromagnetic radiation shielding by intrinsically conducting polymers, *Appl. Phys. Lett.*, 1994, **65**(18), 2278–2280.

13 M. Faisal and S. Khasim, Broadband electromagnetic shielding and dielectric properties of polyaniline-stannous oxide composites, *J. Mater. Sci.: Mater. Electron.*, 2013, **24**(7), 2202–2210.

14 M. Dar, M. Abdullah, R. K. Kotnala, V. Verma, J. Shah, W. A. Siddiqui and M. Alam, High magneto-crystalline anisotropic core–shell structured Mn0. $5Zn_{0.5}Fe_2O_4$/polyaniline nanocomposites prepared by in situ emulsion polymerization, *J. Phys. Chem. C*, 2012, **116**(9), 5277–5287.

15 I. D. Mall, V. C. Srivastava, G. V. A. Kumar and I. M. Mishra, Characterization and utilization of mesoporous fertilizer plant waste carbon for adsorptive removal of dyes from aqueous solution, *Colloids Surf., A*, 2006, **278**(1–3), 175–187.

16 P. Singh, V. K. Babbar, A. Razdan, S. L. Srivastava and R. K. Puri, Complex permeability and permittivity, and microwave absorption studies of Ca (CoTi) xFe12− 2xO19 hexaferrite composites in X-band microwave frequencies, *Mater. Sci. Eng., B*, 1999, **67**(3), 132–138.

17 P. Saini, V. Choudhary, B. P. Singh, R. B. Mathur and S. K. Dhawan, Polyaniline–MWCNT nanocomposites for microwave absorption and EMI shielding, *Mater. Chem. Phys.*, 2009, **113**(2–3), 919–926.

18 S. Mishra, P. Chaudhary, B. C. Yadav, A. Umar, P. Lohia and D. K. Dwivedi, Fabrication and characterization of an ultrasensitive humidity sensor based on chalcogenide glassy alloy thin films, *Eng. Sci.*, 2021, **15**, 138–147.

19 J. Yan, H. Wei, H. Xie, X. Gu and H. Bao, Seeking for low thermal conductivity atomic configurations in SiGe alloys with bayesian optimization, *ES Energy Environ.*, 2020, **8**(3), 56–64.

20 T. Xin, Y. Zhao, R. Mahjoub, J. Jiang, A. Yadav, K. Nomoto and R. Niu, Ultrahigh specific strength in a magnesium alloy strengthened by spinodal decomposition, *Sci. Adv.*, 2021, **7**(23), eabf3039.

21 L. Chen, Y. Zhao, M. Li, L. Li, L. Hou and H. Hou, Reinforced AZ91D magnesium alloy with thixomolding process facilitated dispersion of graphene nanoplatelets and enhanced interfacial interactions, *Mater. Sci. Eng., A*, 2021, **804**, 140793.

22 Z. H. A. O. YuHong, J. I. N. G. JianHui, C. H. E. N. Liwen and H. O. U. Hua, Current Research Status of Interface of Ceramic-Metal Laminated Composite Material for Armor Protection, *Acta Metall. Sin.*, 2021, **57**(9), 1107–1125.

23 J. Gu, Y. Li, C. Liang, Y. Tang, L. Tang, Y. Zhang, J. Kong, H. Liu and Z. Guo, Synchronously improved dielectric and mechanical properties of wave-transparent laminated composites combined with outstanding thermal stability by incorporating iysozyme/POSS functionalized PBO fibers, *J. Mater. Chem. C*, 2018, **6**(28), 7652–7660.

24 N. Wu, C. Liu, D. Xu, J. Liu, W. Liu, Q. Shao and Z. Guo, Enhanced electromagnetic wave absorption of three-dimensional porous Fe_3O_4/C composite flowers, *ACS Sustainable Chem. Eng.*, 2018, **6**(9), 12471–12480.

25 Y. Song, L. He, X. Zhang, F. Liu, N. Tian, Y. Tang and J. Kong, Highly efficient electromagnetic wave absorbing metal-free and carbon-rich ceramics derived from hyperbranched polycarbosilazanes, *J. Phys. Chem. C*, 2017, **121**(44), 24774–24785.

26 C. Luo, W. Duan, X. Yin and J. Kong, Microwave-absorbing polymer-derived ceramics from cobalt-coordinated poly (dimethylsilylene) diacetylenes, *J. Phys. Chem. C*, 2016, **120**(33), 18721–18732.

27 C. C. Yang, Y. J. Gung, W. C. Hung, T. H. Ting and K. H. Wu, Infrared and microwave absorbing properties of $BaTiO_3$/polyaniline and $BaFe_{12}O_{19}$/polyaniline composites, *Compos. Sci. Technol.*, 2010, **70**(3), 466–471.

28 M.-S. Cao, X.-X. Wang, W.-Q. Cao and J. Yuan, Ultrathin graphene: electrical properties and highly efficient electromagnetic interference shielding, *J. Mater. Chem. C*, 2015, **3**(26), 6589–6599.

29 C. Xiang, Y. Pan, X. Liu, X. Sun, X. Shi and J. Guo, Microwave attenuation of multiwalled carbon nanotube-fused silica composites, *Appl. Phys. Lett.*, 2005, **87**(12), 123103.

30 R. Kumar, A. Kumar and D. Kumar, RFI/EMI/microwave shielding behaviour of metallized fabric-a theoretical approach, Proceedings of the International Conference

on Electromagnetic Interference and Compatibility' (IEEE Cat. No. 99TH 8487), 1997, vol. 99, pp. 447-450.
31 P. Saini, V. Choudhary, B. P. Singh, R. B. Mathur and S. K. Dhawan, Enhanced microwave absorption behavior of polyaniline-CNT/polystyrene blend in 12.4–18.0 GHz range, *Synth. Met.*, 2011, **161**(15–16), 1522–1526.
32 M. B. Bryning, B. Mateusz, M. F. Islam, J. M. Kikkawa and A. G. Yodh, Very low conductivity threshold in bulk isotropic single-walled carbon nanotube–epoxy composites, *Adv. Mater.*, 2005, **17**(9), 1186–1191.
33 M. H. Al-Saleh and U. Sundararaj, A review of vapor grown carbon nanofiber/polymer conductive composites, *Carbon*, 2009, **47**(1), 2–22.
34 N. C. Das, D. Khastgir, T. K. Chaki and A. Chakraborty, Electromagnetic interference shielding effectiveness of carbon black and carbon fibre filled EVA and NR based composites, *Composites, Part A*, 2000, **31**(10), 1069–1081.
35 N. C. Das, T. K. Chaki, D. Khastgir and A. Chakraborty, Electromagnetic interference shielding effectiveness of conductive carbon black and carbon fiber-filled composites based on rubber and rubber blends, *Adv. Polym. Technol.*, 2001, **20**(3), 226–236.
36 S. H. Park, P. Thielemann, P. Asbeck and P. R. Bandaru, Enhanced dielectric constants and shielding effectiveness of, uniformly dispersed, functionalized carbon nanotube composites, *Appl. Phys. Lett.*, 2009, **94**(24), 243111.
37 B. Yuan, L. Yu, L. Sheng, K. An and X. Zhao, Comparison of electromagnetic interference shielding properties between single-wall carbon nanotube and graphene sheet/polyaniline composites, *J. Phys. D: Appl. Phys.*, 2012, **45**(23), 235108.
38 D. Micheli, R. Pastore, C. Apollo, M. Marchetti, G. Gradoni, F. Moglie and V. M. Primiani, Carbon based nanomaterial composites in RAM and microwave shielding applications, 9th IEEE Conference on Nanotechnology (IEEE-NANO), IEEE, 2009, pp. 226-235.
39 H. Xu, S. M. Anlage, L. Hu and G. Gruner, Microwave shielding of transparent and conducting single-walled carbon nanotube films, *Appl. Phys. Lett.*, 2007, **90**(18), 183119.
40 U. Basuli, S. Chattopadhyay, C. Nah and T. K. Chaki, Electrical properties and electromagnetic interference shielding effectiveness of multiwalled carbon nanotubes-reinforced EMA nanocomposites, *Polym. Compos.*, 2012, **33**(6), 897–903.
41 M. Arjmand, T. Apperley, M. Okoniewski and U. Sundararaj, Comparative study of electromagnetic interference shielding properties of injection molded versus compression molded multi-walled carbon nanotube/polystyrene composites, *Carbon*, 2012, **50**(14), 5126–5134.
42 A. Gupta and V. Choudhary, Electrical conductivity and shielding effectiveness of poly (trimethylene terephthalate)/multiwalled carbon nanotube composites, *J. Mater. Sci.*, 2011, **46**(19), 6416–6423.
43 R. Ravindren, S. Mondal, K. Nath and N. C. Das, Synergistic effect of double percolated co-supportive MWCNT-CB conductive network for high-performance EMI shielding application, *Polym. Adv. Technol.*, 2019, **30**(6), 1506–1517.
44 H. M. Kim, K. Kim, C. Y. Lee, J. Joo, S. J. Cho, H. S. Yoon, D. A. Pejaković, J.-W. Yoo and A. J. Epstein, Electrical conductivity and electromagnetic interference shielding of multiwalled carbon nanotube composites containing Fe catalyst, *Appl. Phys. Lett.*, 2004, **84**(4), 589–591.
45 W.-L. Song, C. Gong, H. Li, X.-D. Cheng, M. Chen, X. Yuan, H. Chen, Y. Yang and D. Fang, Graphene-based sandwich structures for frequency selectable electromagnetic shielding, *ACS Appl. Mater. Interfaces*, 2017, **9**(41), 36119–36129.
46 N. Gill, V. Gupta, M. Tomar, A. L. Sharma, O. P. Pandey and D. P. Singh, Improved electromagnetic shielding behaviour of graphene encapsulated polypyrrole-graphene nanocomposite in X-band, *Compos. Sci. Technol.*, 2020, **192**, 108113.
47 A. A. Khodiri, M. Y. Al-Ashry and A. G. El-Shamy, Novel hybrid nanocomposites based on polyvinyl alcohol/graphene/magnetite nanoparticles for high electromagnetic shielding performance, *J. Alloys Compd.*, 2020, **847**, 156430.
48 S. Kashi, R. K. Gupta, T. Baum, N. Kao and S. N. Bhattacharya, Dielectric properties and electromagnetic interference shielding effectiveness of graphene-based biodegradable nanocomposites, *Mater. Des.*, 2016, **109**, 68–78.
49 J. Noto, G. Fenical and C. Tong, Automotive EMI shielding–controlling automotive electronic emissions and susceptibility with proper EMI suppression methods, URL: https://www.lairdtech.com/sites/default/files/public/solutions/Laird-EMI-WP-Automotive-EMI-Shielding-040114.Pdf, 2010.
50 S. R. Dhakate and K. M. Subhedar, and Bhanu Pratap Singh, Polymer nanocomposite foam filled with carbon nanomaterials as an efficient electromagnetic interference shielding material, *RSC Adv.*, 2015, **5**(54), 43036–43057.
51 M. H. Al-Saleh and U. Sundararaj, Electromagnetic interference shielding mechanisms of CNT/polymer composites, *Carbon*, 2009, **47**(7), 1738–1746.
52 S. Biswas, G. P. Kar and S. Bose, Engineering nanostructured polymer blends with controlled nanoparticle location for excellent microwave absorption: a compartmentalized approach, *Nanoscale*, 2015, **7**(26), 11334–11351.
53 K. L. Kaiser, *Electromagnetic shielding*, Crc Press, 2005.
54 J. Liang, Y. Wang, Y. Huang, Y. Ma, Z. Liu, J. Cai, C. Zhang, H. Gao and Y. Chen, Electromagnetic interference shielding of graphene/epoxy composites, *Carbon*, 2009, **47**(3), 922–925.
55 J.-C. Shu, W.-Q. Cao and M.-S. Cao, Diverse Metal–Organic Framework Architectures for Electromagnetic Absorbers and Shielding, *Adv. Funct. Mater.*, 2021, 2100470.
56 M.-S. Cao, J.-C. Shu, B. Wen, X.-X. Wang and W.-Q. Cao, Genetic Dielectric Genes Inside 2D Carbon-Based Materials with Tunable Electromagnetic Function at Elevated Temperature, *Small Struct.*, 2021, **2**(11), 2100104.
57 X.-X. Wang, J.-C. Shu, W.-Q. Cao, M. Zhang, J. Yuan and M.-S. Cao, Eco-mimetic nanoarchitecture for green EMI shielding, *Chem. Eng. J.*, 2019, **369**, 1068–1077.
58 X.-X. Wang, M. Zhang, J.-C. Shu, B. Wen, W.-Q. Cao and M.-S. Cao, Thermally-tailoring dielectric ''genes'' in

graphene-based heterostructure to manipulate electromagnetic response, *Carbon*, 2021, **184**, 136–145.
59 V. Shukla, Review of electromagnetic interference shielding materials fabricated by iron ingredients, *Nanoscale Adv.*, 2019, **1**(5), 1640–1671.
60 V. Shukla and S. K. Srivastava, Reduced graphene oxide/PdNi/poly (ethylene-co vinyl acetate) nanocomposites for electromagnetic interference shielding, *Mater. Chem. Phys.*, 2021, 125418.
61 B. Wen, M. Cao, M. Lu, W. Cao, H. Shi, J. Liu and X. Wang, Reduced graphene oxides: light-weight and high-efficiency electromagnetic interference shielding at elevated temperatures, *Adv. Mater.*, 2014, **26**(21), 3484–3489.
62 M. Cao, X. Wang, W. Cao, X. Fang, B. Wen and J. Yuan, Thermally driven transport and relaxation switching self-powered electromagnetic energy conversion, *Small*, 2018, **14**(29), 1800987.
63 N. Wu, B. Zhao, J. Liu, Y. Li, Y. Chen, L. Chen, M. Wang and Z. Guo, MOF-derived porous hollow Ni/C composites with optimized impedance matching as lightweight microwave absorption materials, *Adv. Compos. Hybrid Mater.*, 2021, **4**(3), 707–715.
64 P. Xie, Y. Liu, M. Feng, M. Niu, C. Liu, N. Wu and K. Sui, Hierarchically porous Co/C nanocomposites for ultralight high-performance microwave absorption, *Adv. Compos. Hybrid Mater.*, 2021, **4**(1), 173–185.
65 N. Wu, W. Du, Q. Hu and S. V. Q. Jiang, Recent development in fabrication of Co nanostructures and their carbon nanocomposites for electromagnetic wave absorption, *Eng. Sci.*, 2020, **13**(13), 11–23.
66 H. Cheng, Z. Lu, Q. Gao, Y. Zuo, X. Liu, Z. Guo, C. Liu and C. Shen, PVDF-Ni/PE-CNTs composite foams with co-continuous structure for electromagnetic interference shielding and photo-electro-thermal properties, *Eng. Sci.*, 2021, **16**, 331–340.
67 N. F. Colaneri and L. W. Schacklette, EMI shielding measurements of conductive polymer blends, *IEEE Trans. Instrum. Meas.*, 1992, **41**(2), 291–297.
68 X. Luo and D. D. L. Chung, Electromagnetic interference shielding using continuous carbon-fiber carbon-matrix and polymer-matrix composites, *Composites, Part B*, 1999, **30**(3), 227–231.
69 M. M. Abdi, A. B. Kassim, H. N. M. Ekramul Mahmud, W. M. M. Yunus and Z. A. Talib, Electromagnetic interference shielding effectiveness of new conducting polymer composite, *J. Macromol. Sci., Part A: Pure Appl. Chem.*, 2009, **47**(1), 71–75.
70 Vikas Rathi, and Varij Panwar, *Electromagnetic interference shielding analysis of conducting composites in near-and far-field region*, IEEE Trans. Electromagn. Compat., 2018, **60**(6), 1795–1801.
71 D. D. Chung, Materials for electromagnetic interference shielding, *Mater. Chem. Phys.*, 2020, 123587.
72 P. Saini and M. Arora, Microwave absorption and EMI shielding behavior of nanocomposites based on intrinsically conducting polymers, graphene and carbon nanotubes, *New polymers for special applications*, InTech, Croatia, 2012, vol. 3, pp. 71–112.
73 W.-Y. Chiang and Y.-S. Chiang, Effect of titanate coupling agent on electromagnetic interference shielding effectiveness and mechanical properties of PC–ABS–NCF composite, *J. Appl. Polym. Sci.*, 1992, **46**(4), 673–681.
74 V. Panwar and R. M. Mehra, Analysis of electrical, dielectric, and electromagnetic interference shielding behavior of graphite filled high density polyethylene composites, *Polym. Eng. Sci.*, 2008, **48**(11), 2178–2187.
75 V. Eswaraiah, V. Sankaranarayanan and S. Ramaprabhu, Functionalized graphene–PVDF foam composites for EMI shielding, *Macromol. Mater. Eng.*, 2011, **296**(10), 894–898.
76 S. Shinagawa, Y. Kumagai and K. Urabe, Conductive papers containing metallized polyester fibers for electromagnetic interference shielding, *J. Porous Mater.*, 1999, **6**(3), 185–190.
77 D. D. L. Chung, *Composite materials for electromagnetic applications, Composite Materials*, Springer, 2003, pp. 91–99.
78 Z. Zeng, H. Jin, M. Chen, W. Li, L. Zhou and Z. Zhang, Lightweight and anisotropic porous MWCNT/WPU composites for ultrahigh performance electromagnetic interference shielding, *Adv. Funct. Mater.*, 2016, **26**(2), 303–310.
79 A. Colin, M. Perotoni, K. Marconi, E. Ferreira, M. Andrade, S. Marchiori, M. Menezes and A. Nogueira, Feature selective validation analysis applied to measurement and simulation of electronic circuit electromagnetic emissions, 2017 International Symposium on Electromagnetic Compatibility-EMC EUROPE, IEEE, 2017, pp. 1–6.
80 F. Wu, Y. Xia, Y. Wang and M. Wang, Two-step reduction of self-assembed three-dimensional (3D) reduced graphene oxide (RGO)/zinc oxide (ZnO) nanocomposites for electromagnetic absorption, *J. Mater. Chem. A*, 2014, **2**(47), 20307–20315.
81 R. Strumpler and J. Glatz-Reichenbach, Conducting polymer composites, *J. Electroceram.*, 1999, **3**(4), 329–346.
82 B. Adamczyk, *Foundations of Electromagnetic Compatibility: with Practical Applications*, John Wiley & Sons, 2017.
83 Z. Liu, G. Bai, Y. Huang, Y. Ma, F. Du, F. Li, T. Guo and Y. Chen, Reflection and absorption contributions to the electromagnetic interference shielding of single-walled carbon nanotube/polyurethane composites, *Carbon*, 2007, **45**(4), 821–827.
84 D. H. Park, D. Hyup, Y. K. Lee, S. S. Park, C. S. Lee, S. H. Kim and W. N. Kim, Effects of hybrid fillers on the electrical conductivity and EMI shielding efficiency of polypropylene/conductive filler composites, *Macromol. Res.*, 2013, **21**(8), 905–910.
85 G. Jose and P. V. Padeep, Electromagnetic shielding effectiveness and mechanical characteristics of polypropylene based CFRP, *International Journal on Theoretical and Applied Research in Mechanical Engineering (IJTARME)*, 2014, **3**(3), 47–53.
86 S. Mondal, P. Das, S. Ganguly, R. Ravindren, S. Remanan, P. Bhawal, T. K. Das and N. C. Das, Thermal-air ageing treatment on mechanical, electrical, and electromagnetic

interference shielding properties of lightweight carbon nanotube based polymer nanocomposites, *Composites, Part A*, 2018, **107**, 447–460.

87 E. Logakis, C. Pandis, V. Peoglos, P. Pissis, J. Pionteck, P. Pötschke, M. Mičušík and M. Omastová, Electrical/dielectric properties and conduction mechanism in melt processed polyamide/multi-walled carbon nanotubes composites, *Polymer*, 2009, **50**(21), 5103–5111.

88 N. Hu, Z. Masuda, G. Yamamoto, H. Fukunaga, T. Hashida and J. Qiu, Effect of fabrication process on electrical properties of polymer/multi-wall carbon nanotube nanocomposites, *Composites, Part A*, 2008, **39**(5), 893–903.

89 G. A. Gelves, M. H. Al-Saleh and U. Sundararaj, Highly electrically conductive and high performance EMI shielding nanowire/polymer nanocomposites by miscible mixing and precipitation, *J. Mater. Chem.*, 2011, **21**(3), 829–836.

90 M. Koledintseva, J. Drewniak, R. DuBroff, K. Rozanov and B. Archambeault, Modeling of shielding composite materials and structures for microwave frequencies, *Prog. Electromagn. Res. B*, 2009, **15**, 197–215.

91 F. D. Paulis, M. H. Nisanci, M. Koledintseva, J. Drewniak and A. Orlandi, Homogenized permittivity of composites with aligned cylindrical inclusions for causal electromagnetic simulations, *Prog. Electromagn. Res. B*, 2012, **37**, 205–235.

92 D. Micheli, R. Pastore, A. Vricella, A. Delfini, M. Marchetti and F. Santoni, Electromagnetic characterization of materials by vector network analyzer experimental setup, *Spectroscopic Methods for Nanomaterials Characterization*, Elsevier, 2017, pp. 195–236.

93 S. Sankaran, K. Deshmukh, M. B. Ahamed and S. K. K. Pasha, Recent advances in electromagnetic interference shielding properties of metal and carbon filler reinforced flexible polymer composites: a review, *Composites, Part A*, 2018, **114**, 49–71.

94 S. Colak, D. Varevac and I. Milicevic, Materials that improve the shielding efficiency from em radiation, *Ann. DAAAM Proc.*, 2020, **7**, 1.

95 M. González, J. Pozuelo and J. Baselga, Electromagnetic shielding materials in GHz range, *Chem. Rec.*, 2018, **18**(7-8), 1000–1009.

96 J. Margineda, G. J. Molina-Cuberos, M. J. Núñez, A. J. García-Collado and E. Martín, Electromagnetic characterization of chiral media, *Solutions and Applications of Scattering, Propagation, Radiation and Emission of Electromagnetic Waves*, Intech Open, 2012.

97 B. Mensah, H. G. Kim, J.-H. Lee, S. Arepalli and C. Nah, Carbon nanotube-reinforced elastomeric nanocomposites: a review, *Int. J. Smart Nano Mater.*, 2015, **6**(4), 211–238.

98 M. Zahid, Y. Nawab, N. Gulzar, Z. A. Rehan, M. F. Shakir, A. Afzal, I. A. Rashid and A. Tariq, Fabrication of reduced graphene oxide (RGO) and nanocomposite with thermoplastic polyurethane (TPU) for EMI shielding application, *J. Mater. Sci.: Mater. Electron.*, 2020, **31**(2), 967–974.

99 Q. Jiang, X. Liao, J. Li, J. Chen, G. Wang, J. Yi, Q. Yang and G. Li, Flexible thermoplastic polyurethane/reduced graphene oxide composite foams for electromagnetic interference shielding with high absorption characteristic, *Composites, Part A*, 2019, **123**, 310–319.

100 Y. Li, B. Shen, D. Yi, L. Zhang, W. Zhai, X. Wei and W. Zheng, The influence of gradient and sandwich configurations on the electromagnetic interference shielding performance of multi-layered thermoplastic polyurethane/graphene composite foams, *Compos. Sci. Technol.*, 2017, **138**, 209–216.

101 S. Kuester, N. R. Demarquette, J. C. Ferreira Jr., B. G. Soares and G. M. Barra, Hybrid nanocomposites of thermoplastic elastomer and carbon nanoadditives for electromagnetic shielding, *Eur. Polym. J.*, 2017, **88**, 328–339.

102 S. Kuester, G. M. Barra, J. C. Ferreira Jr, B. G. Soares and N. R. Demarquette, Electromagnetic interference shielding and electrical properties of nanocomposites based on poly (styrene-*b*-ethylene-ran-butylene-*b*-styrene) and carbon nanotubes, *Eur. Polym. J.*, 2016, **77**, 43–53.

103 C. Liu, W. Wu, Y. Wang, Z. Wang and Q. Chen, Silver-coated thermoplastic polyurethane hybrid granules for dual-functional elastomer composites with exceptional thermal conductive and electromagnetic interference shielding performances, *Compos. Commun.*, 2021, **25**, 100719.

104 Y. Zhan, J. Wang, K. Zhang, Y. Li, Y. Meng, N. Yan, W. Wei, F. Peng and H. Xia, Fabrication of a flexible electromagnetic interference shielding Fe_3O_4@ reduced graphene oxide/natural rubber composite with segregated network, *Chem. Eng. J.*, 2018, **344**, 184–193.

105 N. R. Choudhury and A. K. Bhowmick, Strength of thermoplastic elastomers from rubber-polyolefin blends, *J. Mater. Sci.*, 1990, **25**(1), 161–167.

106 N. R. Legge, Thermoplastic Elastomers, *Rubber Chem. Technol.*, 1987, **60**(3), 83–117.

107 H. L. Stephens and A. K. Bhowmick, *Handbook of Elastomers*, Dekker, 2001.

108 B. M. Walker and C. P. Rader, *Handbook of thermoplastic elastomers*, Van Nostrand Reinhold, New York, 1979.

109 J. T. Bailey, E. T. Bishop and W. R. Hendricks, Rubber Age, 98, 69 (1966), CAS AW Van Breen M Vlig, Rubber Plast Age 1966, 47,1070.

110 K. William, *Fischer Thermoplastic blend of partially cured monoolefin copolymer rubber and polyolefin plastic*. US Pat. US366927A, 1975.

111 D. R. Paul, Control of phase structure in polymer blends, *Functional Polymer*, Springer, 1989, pp. 1–18.

112 P. Nevatia, T. S. Banerjee, B. Dutta, A. Jha, A. K. Naskar and A. K. Bhowmick, Thermoplastic elastomers from reclaimed rubber and waste plastics, *J. Appl. Polym. Sci.*, 2002, **83**(9), 2035–2042.

113 S. K. De and A. K. Bhowmick, *Thermoplastic elastomers from rubber-plastic blends*, Ellis Horwood Limited, 1990.

114 A. Fazli and D. Rodrigue, Waste Rubber Recycling: A Review on the Evolution and Properties of Thermoplastic Elastomers, *Materials*, 2020, **13**, 782.

115 A. Lv, X.-X. Deng, L. Li, Z.-L. Li, Y.-Z. Wang, F.-S. Du and Z.-C. Li, Facile synthesis of multi-block copolymers containing poly (ester–amide) segments with an ordered side group sequence, *Polym. Chem.*, 2013, **4**(13), 3659–3662.

116 G. Acik, H. R. F. Karabulut, C. Altinkok and A. O. Karatavuk, Synthesis and characterization of biodegradable polyurethanes made from cholic acid and l-lysine diisocyanate ethyl ester, *Polym. Degrad. Stab.*, 2019, **165**, 43–48.

117 G. Acik, Soybean oil modified bio-based poly (vinyl alcohol) s via ring-opening polymerization, *J. Polym. Environ.*, 2019, **27**(11), 2618–2623.

118 A. K. Naskar, S. K. De and A. K. Bhowmick, Thermoplastic elastomeric composition based on maleic anhydride–grafted ground rubber tire, *J. Appl. Polym. Sci.*, 2002, **84**(2), 370–378.

119 A. Ganguly, M. De Sarkar and A. K. Bhowmick, Thermoplastic elastomeric nanocomposites from poly[styrene-(ethylene-*co*-butylene)-styrene] triblock copolymer and clay: Preparation and characterization, *J. Appl. Polym. Sci.*, 2006, **100**, 2040–2052.

120 A. Jha and A. K. Bhowmick, Thermal degradation and ageing behaviour of novel thermoplastic elastomeric nylon-6/acrylate rubber reactive blends, *Polym. Degrad. Stab.*, 1998, **62**, 575–586.

121 N. R. Legge, Thermoplastic Elastomers—Three Decades of Progress, *Rubber Chem. Technol.*, 1989, **62**, 529–547.

122 S. Kuester, C. Merlini, G. M. Barra, J. C. Ferreira Jr., A. Lucas, A. Cristina de Souza and B. G. Soares, Processing and characterization of conductive composites based on poly (styrene-*b*-ethylene-ran-butylene-*b*-styrene) (SEBS) and carbon additives: A comparative study of expanded graphite and carbon black, *Composites, Part B*, 2016, **84**, 236–247.

123 Y. Xu, S. Tang, J. Pan, J. Bao and A. Zhang, Reversibly cross-linked SEBS/carbon hybrid composite with excellent solvent-proof and electromagnetic shielding properties, *Mater. Des.*, 2018, **146**, 1–11.

124 W. M. Albers, M. Karttunen, L. Wikström and T. Vilkman, Effects of compression and filler particle coating on the electrical conductivity of thermoplastic elastomer composites, *J. Electron. Mater.*, 2013, **42**(10), 2983–2989.

125 J. Pan, J. Yue and J. Bao, Flexible poly(styrene-*b*-(ethylene-*co*-butylene)-*b*-styrene) nanocomposites for electromagnetic interference shielding, *J. Appl. Polym. Sci.*, 2020, **137**(14), 48542.

126 S. Zhao, P. P. Sun, X. Shao, X. Liu, Z. Zhao, L. Li and Z. Xin, ZrO2 functionalized graphene Oxide/SEBS-Based nanocomposites for efficient electromagnetic interference shielding applications, *J. Vinyl Addit. Technol.*, 2019, **25**(S1), E130–E136.

127 D. Tian, Y. Wang, Y. Xu, L. Zhang, Y. Hu, F. Deng and R. Sun, A conductive composite foam based on poly(styrene-butadiene-styrene)/carbon nanotube (SBS/CNT) for electromagnetic interference shielding, 2020 21st International Conference on Electronic Packaging Technology (ICEPT), IEEE, 2020, pp. 1–5.

128 J. R. Flesher, Pebax® polyether block amide—A new family of engineering thermoplastic elastomers, *High performance polymers: their origin and development*, Springer, Dordrecht, 1986, pp. 401–408.

129 D. Wang, S. Song, W. Zhang, Z. He, Y. Wang, Y. Zheng and D. Yao, CO_2 selective separation of Pebax-based mixed matrix membranes (MMMs) accelerated by silica nanoparticle organic hybrid materials (NOHMs), *Sep. Purif. Technol.*, 2020, **241**, 116708.

130 X. Wang, X. Ding, H. Zhao, J. Fu, Q. Xin and Y. Zhang, Pebax-based mixed matrix membranes containing hollow polypyrrole nanospheres with mesoporous shells for enhanced gas permeation performance, *J. Membr. Sci.*, 2020, **602**, 117968.

131 C. Ge, G. Wang, G. Zhao, C. Wei and X. Li, Lightweight and flexible poly(ether-*block*-amide)/multiwalled carbon nanotube composites with porous structure and segregated conductive networks for electromagnetic shielding applications, *Composites, Part A*, 2021, **144**, 106356.

132 G. Wang, J. Zhao, C. Ge, G. Zhao and C. B. Park, Nanocellular poly(ether-*block*-amide)/MWCNT nanocomposite films fabricated by stretching-assisted microcellular foaming for high-performance EMI shielding applications, *J. Mater. Chem. C*, 2021, **9**(4), 1245–1258.

133 B. Zhao, X. Zhang, J. Deng, C. Zhang, Y. Li, X. Guo and R. Zhang, Flexible PEBAX/graphene electromagnetic shielding composite films with a negative pressure effect of resistance for pressure sensors applications, *RSC Adv.*, 2020, **10**(3), 1535–1543.

134 J. G. Drobny, *Handbook of thermoplastic elastomers*, Elsevier, 2014.

135 N. H. Park, D. H. Kim, K. Y. Kim, D. Y. Lim and H. Ham, Electrical properties of novel polyolefin based thermoplastic elastomer and graphene nanocomposites, *Fibers Polym.*, 2013, **14**(12), 2117–2121.

136 Y.-F. Liu, L.-M. Feng, Y.-F. Chen, Y.-D. Shi, X.-D. Chen and M. Wang, Segregated polypropylene/cross-linked poly(ethylene-*co*-1-octene)/multi-walled carbon nanotube nanocomposites with low percolation threshold and dominated negative temperature coefficient effect: Towards electromagnetic interference shielding and thermistors, *Compos. Sci. Technol.*, 2018, **159**, 152–161.

137 D. H. Park, Y. K. Lee, S. S. Park, C. S. Lee, S. H. Kim and W. N. Kim, Effects of hybrid fillers on the electrical conductivity and EMI shielding efficiency of polypropylene/conductive filler composites, *Macromol. Res.*, 2013, **21**(8), 905–910.

138 L. C. Jia, D.-X. Yan, C.-H. Cui, X. Jiang, X. Ji and Z.-M. Li, Electrically conductive and electromagnetic interference shielding of polyethylene composites with devisable carbon nanotube networks, *J. Mater. Chem. C*, 2015, **3**(36), 9369–9378.

139 B. Yang, Y. Pan, Y. Yu, J. Wu, R. Xia, S. Wang and Y. Wang, Filler network structure in graphene nanoplatelet (GNP)-filled polymethyl methacrylate (PMMA) composites: From thermorheology to electrically and thermally conductive properties, *Polym. Test.*, 2020, **89**, 106575.

140 Ö. B. Mergen, E. Umut, E. Arda and S. Kara, A comparative study on the AC/DC conductivity, dielectric and optical properties of polystyrene/graphene nanoplatelets (PS/GNP) and multi-walled carbon nanotube (PS/MWCNT) nanocomposites, *Polym. Test.*, 2020, **90**, 106682.

141 Z. Guo, P. Ren, B. Fu, F. Ren, Y. Jin and Z. Sun, Multilayered graphene-Fe3O4/poly (vinylidene fluoride) hybrid composite films for high-efficient electromagnetic shielding, *Polym. Test.*, 2020, **89**, 106652.

142 A. Huang, X. Peng and L.-S. Turng, In situ fibrillated polytetrafluoroethylene (PTFE) in thermoplastic polyurethane (TPU) via melt blending: Effect on rheological behavior, mechanical properties, and microcellular foamability, *Polymer*, 2018, **134**, 263–274.

143 A. Rostami and M. I. Moosavi, High-performance thermoplastic polyurethane nanocomposites induced by hybrid application of functionalized graphene and carbon nanotubes, *J. Appl. Polym. Sci.*, 2020, **137**(14), 48520.

144 M. Valentini, F. Piana, J. Pionteck, F. R. Lamastra and F. Nanni, Electromagnetic properties and performance of exfoliated graphite (EG)–thermoplastic polyurethane (TPU) nanocomposites at microwaves, *Compos. Sci. Technol.*, 2015, **114**, 26–33.

145 Y.-S. Jun, S. Habibpour, M. Hamidinejad, M. Gyu Park, W. Ahn, A. Yu and C. B. Park, Enhanced electrical and mechanical properties of graphene nano-ribbon/thermoplastic polyurethane composites, *Carbon*, 2021, **174**, 305–316.

146 X. Li, G. Wang, C. Yang, J. Zhao and A. Zhang, Mechanical and EMI shielding properties of solid and microcellular TPU/nanographite composite membranes, *Polym. Test.*, 2021, **93**, 106891.

147 B. Shen, Y. Li, D. Yi, W. Zhai, X. Wei and W. Zheng, Strong flexible polymer/graphene composite films with 3D saw-tooth folding for enhanced and tunable electromagnetic shielding, *Carbon*, 2017, **113**, 55–62.

148 A. N. Esfahani, A. A. Katbab, A. Taeb, L. Simon and M. A. Pope, Correlation between mechanical dissipation and improved X-band electromagnetic shielding capabilities of amine functionalized graphene/thermoplastic polyurethane composites, *Eur. Polym. J.*, 2017, **95**, 520–538.

149 S. Y. Hong, Y. C. Kim, M. Wang, J.-D. Nam and J. Suhr, Anisotropic electromagnetic interference shielding properties of polymer-based composites with magnetically-responsive aligned Fe3O4 decorated reduced graphene oxide, *Eur. Polym. J.*, 2020, **127**, 109595.

150 X. Ji, D. Chen, Q. Wang, J. Shen and S. Guo, Synergistic effect of flame retardants and carbon nanotubes on flame retarding and electromagnetic shielding properties of thermoplastic polyurethane, *Compos. Sci. Technol.*, 2018, **163**, 49–55.

151 X. Ji, D. Chen, J. Shen and S. Guo, Flexible and flame-retarding thermoplastic polyurethane-based electromagnetic interference shielding composites, *Chem. Eng. J.*, 2019, **370**, 1341–1349.

152 B. Fu, P. Ren, Z. Guo, Y. Du, Y. Jin, Z. Sun, Z. Dai and F. Ren, Construction of three-dimensional interconnected graphene nanosheet network in thermoplastic polyurethane with highly efficient electromagnetic interference shielding, *Composites, Part B*, 2021, **215**, 108813.

153 B. Shin, S. Mondal, M. Lee, S. Kim, Y.-I. Huh and C. Nah, Flexible thermoplastic polyurethane-carbon nanotube composites for electromagnetic interference shielding and thermal management, *Chem. Eng. J.*, 2021, **418**, 129282.

154 Q. Jiang, X. Liao, J. Yang, G. Wang, J. Chen, C. Tian and G. Li, A two-step process for the preparation of thermoplastic polyurethane/graphene aerogel composite foams with multi-stage networks for electromagnetic shielding, *Compos. Commun.*, 2020, **21**, 100416.

155 T. Bansala, M. Joshi, S. Mukhopadhyay, R-an Doong and M. Chaudhary, Electrically conducting graphene-based polyurethane nanocomposites for microwave shielding applications in the Ku band, *J. Mater. Sci.*, 2017, **52**(3), 1546–1560.

156 T. Bansala, M. Joshi and S. Mukhopadhyay, Electromagnetic interference shielding behavior of chemically and thermally reduced graphene based multifunctional polyurethane nanocomposites: A comparative study, *J. Appl. Polym. Sci.*, 2019, **136**(25), 47666.

157 M. Verma, P. Verma, S. K. Dhawan and V. Choudhary, Tailored graphene based polyurethane composites for efficient electrostatic dissipation and electromagnetic interference shielding applications, *RSC Adv.*, 2015, **5**(118), 97349–97358.

158 D. Feng, D. Xu, Q. Wang and P. Liu, Highly stretchable electromagnetic interference (EMI) shielding segregated polyurethane/carbon nanotube composites fabricated by microwave selective sintering, *J. Mater. Chem. C*, 2019, **7**(26), 7938–7946.

159 Z. Durmus, A. Durmus, M. Y. Bektay, H. Kavas, I. S. Unver and B. Aktas, Quantifying structural and electromagnetic interference (EMI) shielding properties of thermoplastic polyurethane–carbon nanofiber/magnetite nanocomposites, *J. Mater. Sci.*, 2016, **51**(17), 8005–8017.

160 N. Gulzar, K. Zubair, M. F. Shakir, M. Zahid, Y. Nawab and Z. A. Rehan, Effect on the EMI shielding properties of cobalt ferrites and coal-fly-ash based polymer nanocomposites, *J. Supercond. Novel Magn.*, 2020, **33**(11), 3519–3524.

161 R. Jan, A. Habib, M. A. Akram, I. Ahmad, A. Shah, M. Sadiq and A. Hussain, Flexible, thin films of graphene–polymer composites for EMI shielding, *Mater. Res. Express*, 2017, **4**(3), 035605.

162 R. Jan, A. Saboor, A. N. Khan and I. Ahmad, Estimating EMI shielding effectiveness of graphene-polymer composites at elevated temperatures, *Mater. Res. Express*, 2017, **4**(8), 085605.

163 A. Kasgoz, M. Korkmaz, M. B. Alanalp and A. Durmus, Effect of processing method on microstructure, electrical conductivity and electromagnetic wave interference (EMI) shielding performance of carbon nanofiber filled thermoplastic polyurethane composites, *J. Polym. Res.*, 2017, **24**(9), 1–11.

164 S. D. Ramoa, G. M. Barra, R. V. B. Oliveira, M. G. de Oliveira, M. Cossa and B. G. Soares, Electrical, rheological and electromagnetic interference shielding properties of thermoplastic polyurethane/carbon nanotube composites, *Polym. Int.*, 2013, **62**(10), 1477–1484.

165 J.-M. Thomassin, C. Jerome, T. Pardoen, C. Bailly, I. Huynen and C. Detrembleur, Polymer/carbon based composites as electromagnetic interference (EMI) shielding materials, *Mater. Sci. Eng., R*, 2013, **74**(7), 211–232.

166 F. Goharpey, H. Nazockdast and A. A. Katbab, Relationship between the rheology and morphology of dynamically vulcanized thermoplastic elastomers based on EPDM/PP, *Polym. Eng. Sci.*, 2005, **45**(1), 84–94.

167 K. Shehzad, Z.-M. Dang, M. N. Ahmad, R. U. R. Sagar, S. Butt, M. U. Farooq and T.-B. Wang, Effects of carbon nanotubes aspect ratio on the qualitative and quantitative aspects of frequency response of electrical conductivity and dielectric permittivity in the carbon nanotube/polymer composites, *Carbon*, 2013, **54**, 105–112.

168 M. Mehranvari, A. A. Katbab, V. Nayyeri and H. Nazokdast, Preparation of a radar absorbing material based on PP/EPDM thermoplastic elastomer and carbon nanotube nanocomposite, *Asia-Pacific Microwave Conference (APMC)*, IEEE, 2016, pp. 1–4.

169 H. Duan, M. Zhao, Y. Yang, G. Zhao and Y. Liu, Flexible and conductive PP/EPDM/Ni coated glass fiber composite for efficient electromagnetic interference shielding, *J. Mater. Sci.: Mater. Electron.*, 2018, **29**(12), 10329–10336.

170 L. Ma, W. Yang and C. Jiang, Stretchable conductors of multi-walled carbon nanotubes (MWCNTs) filled thermoplastic vulcanizate (TPV) composites with enhanced electromagnetic interference shielding performance, *Compos. Sci. Technol.*, 2020, **195**, 108195.

171 T. Sharika, J. Abraham, S. C. George, N. Kalarikkal and S. Thomas, Excellent electromagnetic shield derived from MWCNT reinforced NR/PP blend nanocomposites with tailored microstructural properties, *Composites, Part B*, 2019, **173**, 106798.

172 P. Saini and M. Arora, Microwave absorption and EMI shielding behavior of nanocomposites based on intrinsically conducting polymers, graphene and carbon nanotubes, *New polymers for special applications*, InTech, Croatia, 2012, vol. 3, pp. 71–112.